Modelling groundwater vulnerability leveraging a developed Python-coded IDOCRIW-MAUT model in a heterogeneous geologic environment of Nigeria

Soliu Ademola Mudashiru*, Kehinde Anthony Mogaji, Kesyton Oyamenda Ozegin[c]

[a,b]Department of Applied Geophysics, Federal University of Technology, Akure, Nigeria
[c]Department of Physics, Ambrose Alli University Ekpoma, Edo State, Nigeria
*Corresponding Author's Mail: mudashirusa@futa.edu.ng

Authors ORCID IDs: [a]https://orcid.org/0009-0003-2305-9646, [b]https://orcid.org/0000-0001-7069-1319 [c]https://orcid.org/0000-0001-5788-1142

ABSTRACT

Groundwater is a valuable asset for household, farming, and commercial functions and for its ecological benefits. Notwithstanding this, this asset faces a severe threat because of increased contamination from human interference. To guarantee its dependability for current and future usage, groundwater must be managed effectively not solely in regard to availability but also quality. This can be accomplished by pinpointing places that are more susceptible to contamination and adopting countermeasures. The current study used a recently created Python programming-based objective modelling algorithm, the integrated determination of objective criteria weights-multi-attribute utility theory (IDOCIRW-MAUT) modelling algorithm, in evaluating groundwater vulnerability of the study area. The evaluation outputs were contrasted to those established using the analytical hierarchy process (AHP) model. For this evaluation, five groundwater vulnerability modelling factors (GWVBMFs)—bedrock topography, hydraulic conductivity, aquifer depth, drainage density, and slope from geophysical and remote sensing datasets—were weighted applying the IDOCRIW algorithm prior to the ultimate groundwater vulnerability metrics being established by incorporating the weights into the MAUT modelling algorithm. The overall groundwater vulnerability map was created in a GIS context with groundwater vulnerability indices generated by the Python-based IDOCRIW-MAUT modelling program. The groundwater vulnerability evaluation map categorized the research terrain into five kinds: very low, low, medium, medium high, and high groundwater vulnerability, with 3% (59 km²), 26% (485 km²), 33% (608 km²), 25% (473 km²), and 13% (251 km²) falling into each category, respectively. The correlation between the IDOCRIW-MAUT model and the AHP model leveraging longitudinal conductance (LC) data was determined to be 86% and 57%, respectively. The IDOCRIW-MAUT, which used an object-centred framework pattern, is more accurate and has the ability to provide applicable knowledge and potential solutions to choice-making in the field of groundwater quality in the research area and other locations of the globe with similar geologies.

Keywords: Groundwater vulnerability; IDOCRIW-MAUT; Objective MCDM algorithms; Python programming; Ranking of Alternatives; Sensitivity analysis

1. Introduction

Groundwater (GW) remains one of the most significant supplies of water, sustaining household, agricultural-based, and industrial uses (Erostate et al., 2020; Ozegin et al., 2023; Ilugbo et al., 2023; Ozegin et al., 2024a). According to various scholars (Velis et al., 2017; Margat and van der Gun, 2013), groundwater is one of the world's most exploited raw commodities, with a global withdrawal rate of 800-1000 km³/year that exceeds oil by a factor of 20. Consequently, as worldwide consumption of fresh water rises due to population growth and agricultural and commercial development, groundwater serves as a resource that is invaluable in the regular fulfilment of this rising demand (Dangar et al., 2021; Wang et al., 2016). Notwithstanding its global relevance, groundwater remains vulnerable to multiple hazards of contamination across various geologic locations around mankind, including diverse areas where groundwater exists in voids/spaces inside the subsurface, due to a variety of human-caused factors, such as, but not limited to, increased agricultural activities, waste disposal, and urbanization (Gorelick and Zheng, 2015; Jia et al., 2018; Li et al., 2021; Ozegin et al., 2024b). Hence, it is critical to investigate the impact of these activities on groundwater, rendering vulnerability in groundwater modelling a crucial part of groundwater governance (Tavakoli et al., 2024; Allouche et al., 2017).

As stated by Taghavi et al. (2022), groundwater vulnerability (GWVB) describes the degree to which an aquifer is vulnerable to contamination risk, which is impacted by the point and non-point causes of pollution. Pollution from fuelling stations, waste dumps, and sewage treatment plants are examples of point sources, while pollution from non-point sources consists of atmospheric deposition and runoff from farming operations. Groundwater vulnerability is prevalent in the wide-ranging geologic setting known as basement complex areas, as the geologic formation that forms the aquifer system frequently exhibits lower protective capacity resulting from thinner layers of sedimentary overburden layers, which could function as intrinsic filters for contaminants (Kayode et al., 2024). Furthermore, considering the groundwater in these areas is located within voids/cracks in the subsurface, effluents from various pollution sources may seep into them because they house the groundwater and also offer paths for contaminants, rendering groundwater vulnerability in these locations prevalent (Bayewu et al., 2018; Ozegin et al., 2024b).

Numerous researchers have used GIS-based multi-criteria decision-making (MCDM) techniques to model groundwater vulnerability while taking into account a number of criteria and factors from various data sources (Baki et al., 2024; Atenidegbe and Mogaji, 2023; Saqr et al., 2021; Akinwumiju et al., 2018). The complicated decision-making situations associated with groundwater vulnerability modelling have been optimized by using a sequential technique that involves evaluating the various alternatives and allocating weights to influencing parameters (Kumar et al., 2022). Furthermore, these methods facilitate the mapping and spatial analysis of groundwater vulnerability through methodical modelling, which helps to visualize the level of vulnerability risk and support focused groundwater protective measures (Zare et al., 2023).

As important as these models are for groundwater vulnerability modelling, most MCDM approaches (e.g., DRASTIC, Weighted Overlay Method, among others) utilize subjective weight allocation according to expert judgments. Scholars (Sahoo et al., 2023; Şahin, 2021; Parameshwaran et al., 2015) argue that relying on expert judgment can introduce unpredictability and biases, affecting the reliability and generalization of outcomes. The dependence on expert assessments frequently results in inconsistencies in weight allocation due to disparities in individual viewpoints, expertise levels, and differences in methodology. To address these constraints, multiple scholars (Atenidegbe and Mogaji, 2023; Zare et al., 2023; Neshat et al., 2024) implored hybrid and data-driven weighting techniques that use algorithmic objective processes to assign weights based on statistical relationships between criteria, reducing dependency on subjective inputs. These methodologies have so contributed to the optimization of GWVB modelling for enhanced decision-making processes.

Atenidegbe and Mogaji (2023) established the entropy-TOPSIS data mining methods for assessing groundwater risk in a diverse geologic setting, which investigated an objective approach but has its own limitations. One such disadvantage is the use of the entropy weighting model, which has been shown by numerous studies (Zavadskas and Podvezko, 2016; Alao et al., 2021) to result in an overestimation of the objective weights of the criterion. In the context of decision-making, exaggerating the objective weights of the criteria may obscure the true impact of elements, leading some to be discounted while others are assigned an unduly significant consequence. As pointed out by Şahin (2021), this might result in deceptive rankings, as options that should be prioritized may not receive adequate weight evaluation, reducing the dependability of the decision-making process. Apart from weight considerations, the TOPSIS ranking mechanism used introduces another degree of perceived constraint. Because the TOPSIS model uses Euclidean distance to determine proximity to the ideal and negative-ideal solutions, as observed in Chatterjee and Lim's (2022) research, failing to take into account the relative significance of criteria trade-offs during the ranking process may result in biased and incorrect rankings of the options.

To address these limitations, this work used an objective hybrid MCDM model called IDOCRIW-MAUT—integrated determination of objective criteria weights-multi-attribute utility theory—for predicting groundwater vulnerability in a diverse geologic environment. The integrated determination of objective criteria weights (IDOCRIW) provides an enhanced balanced objective weight for the criteria by eliminating the constraint of the entropy weight with the strength of the criteria impact loss (CILOS) model, resulting in a refined objective weight for the criteria (Ayan et al., 2023). According to Çetinkaya et al. (2023), the MAUT model evaluates alternative options based on utility/performance values, accounting for trade-offs among criteria. This leads to efficient ranking of alternatives. Besides, the Python programming language (PPL) was used to assure error-free computing processes because of its wide libraries and robust processing capacity (Aziz et al., 2021). The research area is located in the northern portion of Ondo State, southwestern Nigeria, and is part of a diversified geologic region. The interconnected fractures and discontinuities within the basement complex rocks that comprise this varied geologic region frequently serve as routes for contaminant transportation, making the study area vulnerable to groundwater contamination from surface pollutants caused by a variety of anthropogenic activities such as agricultural wastewater, waste from industries, and ineffective waste disposal. As a result, modelling the study area's groundwater susceptibility is critical for making appropriate groundwater management decisions. The study's goal is to predict the study area's groundwater vulnerability using a Python-coded IDOCRIW-MAUT model that incorporates geophysical and remote sensing characteristics. The study's validated results will thereby help relevant stakeholders make informed decisions about groundwater management in the study area. Furthermore, the scientific approach given here can potentially be used as a reference for future studies both in the study area and in locations with similar geology. This study's uniqueness lies in its use of a Python-coded objective MCDM model, which, according to the reviewed literature, has not previously been reported on for modelling groundwater vulnerability within the study area.

2. Study area description

2.1 General description

The study area is situated in the northern region of Ondo State in southwest Nigeria. It is defined by latitudes 6°55´0´´N to 7°25´0´´N and longitudes 4°50´0´´E to 5°40´0´´E. The study area is 1867 square kilometres in size and is a section of the northern region of Ondo State, which includes five local governments: Ondo East, Ile Oluji, Ifedore, Akure South, Akure North, and parts of Owo (**Fig. 1**). The communities that are situated within the study area have a distinct topography. There is a steady elevation modification, with towns such as Moferere and Fagbo in the southwestern part of the study area having an elevation above sea level (ASL) of 300 m, while towns such as Ijare, Iju, and Igbara Oke in the northern part of the study area have a high elevation of 600 m ASL (Olajide et al., 2020). Furthermore, the study location experiences a tropical climate characterized by distinct wet and dry seasons. The rainy season lasts from April to October and is marked by significant torrential rain that ranges from 1,150 to 2,000 mm per year, whereas the dry season lasts from November to March and has temperatures ranging from 25°C to 29°C, as well as the onset of harmattan season (Omonijo and Matzarakis, 2011). In general, the study region's pedology consists of sandy loam and sandy clay loam, together with lateritic crusts that are frequently found in the few elevated parts of the area.

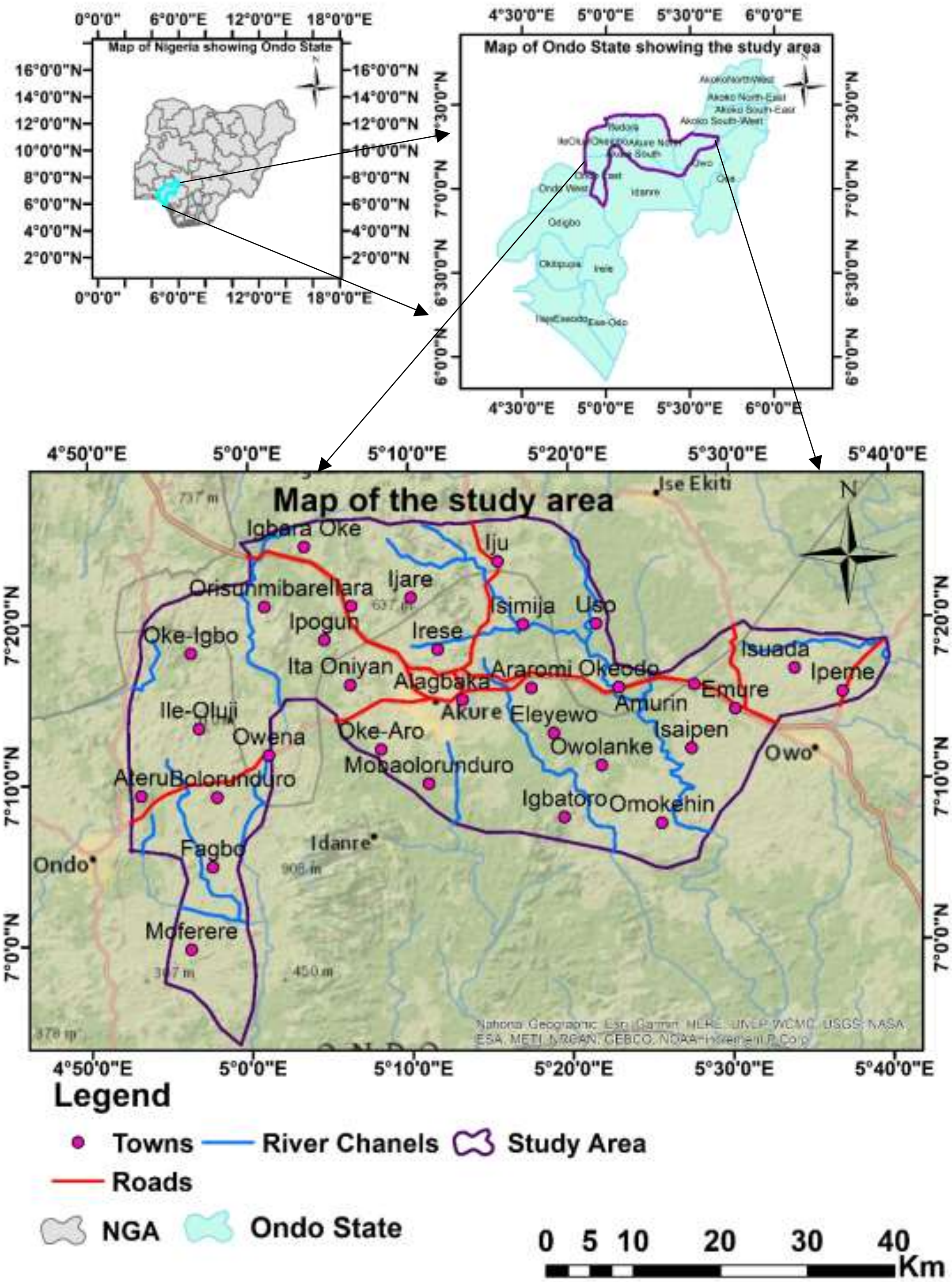

Fig. 1. Location Map of the Study Area showing inset Map of Nigeria and Ondo State.

2.2 Geologic settings

In the context of geology, the research area is underlain by southwestern Nigeria's Precambrian basement complex (Rahaman 1988). The research area contains five primary lithologies: migmatite gneiss, older granite, porphyritic granite, granite gneiss, and biotite granite (**Fig. 2**). Because of their crystalline character, these rock units typically have limited or insignificant primary porosity and permeability, limiting the availability of groundwater to secondary porosity formed during weathering and fracturing (Murray, 2015). As a result, the hydrogeological behaviour of these formations is complex, with important consequences for groundwater sensitivity. Though geologic structures like fractures, faults, and joints increase groundwater availability by acting as conduits for groundwater movement, they also pose a significant risk to groundwater vulnerability. Because these structures act as channels for groundwater movement, pollutants from the surface can quickly permeate through these structural gaps, allowing contaminants to reach deep into aquifer mechanisms in a timely manner (Isah et al., 2025). Furthermore, Vouillamoz et al. (2015) found that the limited aquifer storage capacity in these areas frequently renders natural dilution and attenuation processes less effective, resulting in even minor pollution events having long-term and significant impacts on groundwater quality. Because of the varied geologic diversity of the research area, modelling groundwater risk requires an intricate decision-making process.

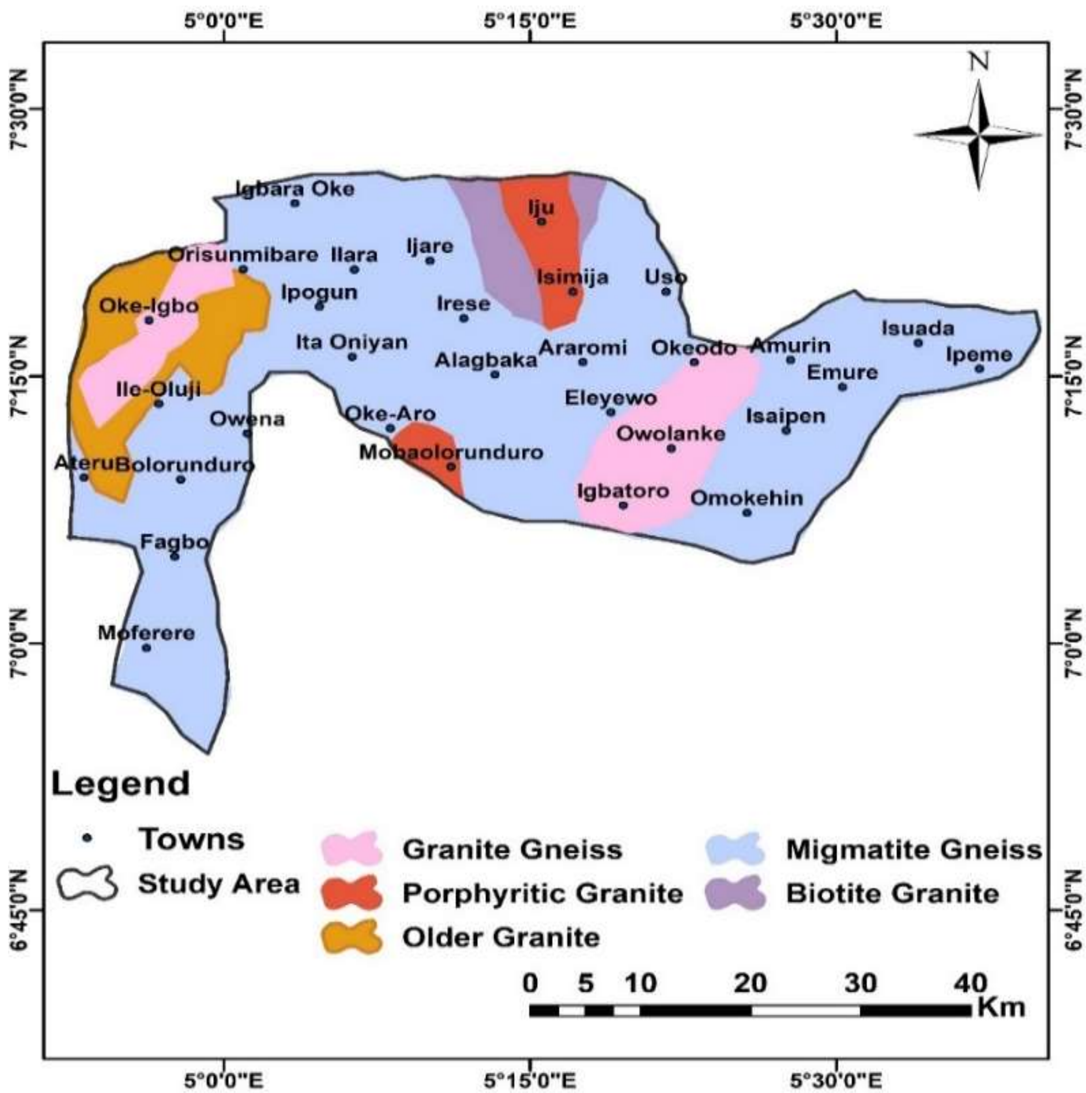

Fig. 2. Geologic Map of the Study Area, modified after NGSA (1996)

3. Data Sources and Methods

3.1 Data sources

The technique begins with the collection, processing, and analysis of important datasets from remote sensing (RS) and geophysical data sources (see **Table 1**). The RS data sets were obtained from the USGS Earth Explorer website (earthexplorer.usgs.gov) and the OpenTopography website (portal.opentopography.org), whereas the geophysical data were obtained from 250 vertical electrical sounding (VES) data points distributed throughout the study area (**Fig. 3**). To use the geophysical datasets in the evaluation, the obtained VES data were interpreted utilizing the partial curve matching approach, followed by computer iterations applying WinResist Version 1.0 software (Vander Velpen, 2004) to produce the depth sounding curves (**Fig. 4**) and further interpretation for estimating the curve type frequency of occurring throughout the research area (**Fig. 5**). The estimated geoelectric layers (**Table 2**) of the research region were then used to calculate the first- and second-order geoelectric variables required for determining the GVMFs. The five factors were selected due to their effectiveness in controlling groundwater penetration, interconnectivity, and flows. These determinants have played an important role in the study at multiple instances. Given that water bodies are not always perennial, rainwater penetration is the primary source of recharge for the aquifer. As a result, the combination of the five variables is especially important in evaluating GVMFs.
Using the digital elevation model (DEM) raster dataset of the study area, which was retrieved from the USGS Earth Explorer Website (earthexplorer.usgs.gov), the DD of the study area was acquired in this study in accordance with the automatic DD creation procedures in ArcGIS 10.7 software. Moreover, the slope of the research region was generated from pre-processed slope raster data from the DEM using the shuttle radar topography mission (SRTM) tool, which has a 30 m resolution and is spread by OpenTopography (portal.opentopography.org).

The HC values of the study area were calculated by employing Eq. 1.

$$HC = 0.0538\exp(-0.0072\rho) \quad (1)$$

where 'h' is the aquifer medium thickness (m), 'ρ' is the aquifer layer resistivity, 'HC' is the hydraulic conductivity (m/day) modified after the hydraulic equation, i.e., $k = 0.0538\exp(-0.0072\rho)$ presented by Mogaji and Atenidegbe (2023).

Consequently, BT was determined using Eq. 2, and values were computed using the Python computer language

$$BT = \text{Elevation (m)} - \text{Depth to Bedrock} \quad (2)$$

Table 1. Details of the data sources employed in the research

GVMFs thematic layers	Data source	Data type	ArcGIS reclassification method
Slope (SL)	Preprocessed slope from OpenTopography	Raster data (continuous) accessed as GeoTIFF	Jenks Natural Break
Drainage Density (DD)	DEM from USGS Earth Explorer	Raster (continuous) accessed as GeoTIFF	Jenks Natural Break
Hydraulic Conductivity (HC)	VES data from electrical resistivity geophysical survey	Vector (point dataset) converted to Raster (interpolation using IDW)	Jenks Natural Break
Aquifer Depth (AD)	VES data from electrical resistivity geophysical survey	Vector (point dataset) converted to Raster (interpolation using IDW)	Jenks Natural Break
Bedrock Topography (BT)	VES data from electrical resistivity geophysical survey	Vector (point dataset) converted to Raster (interpolation using IDW)	Jenks Natural Break

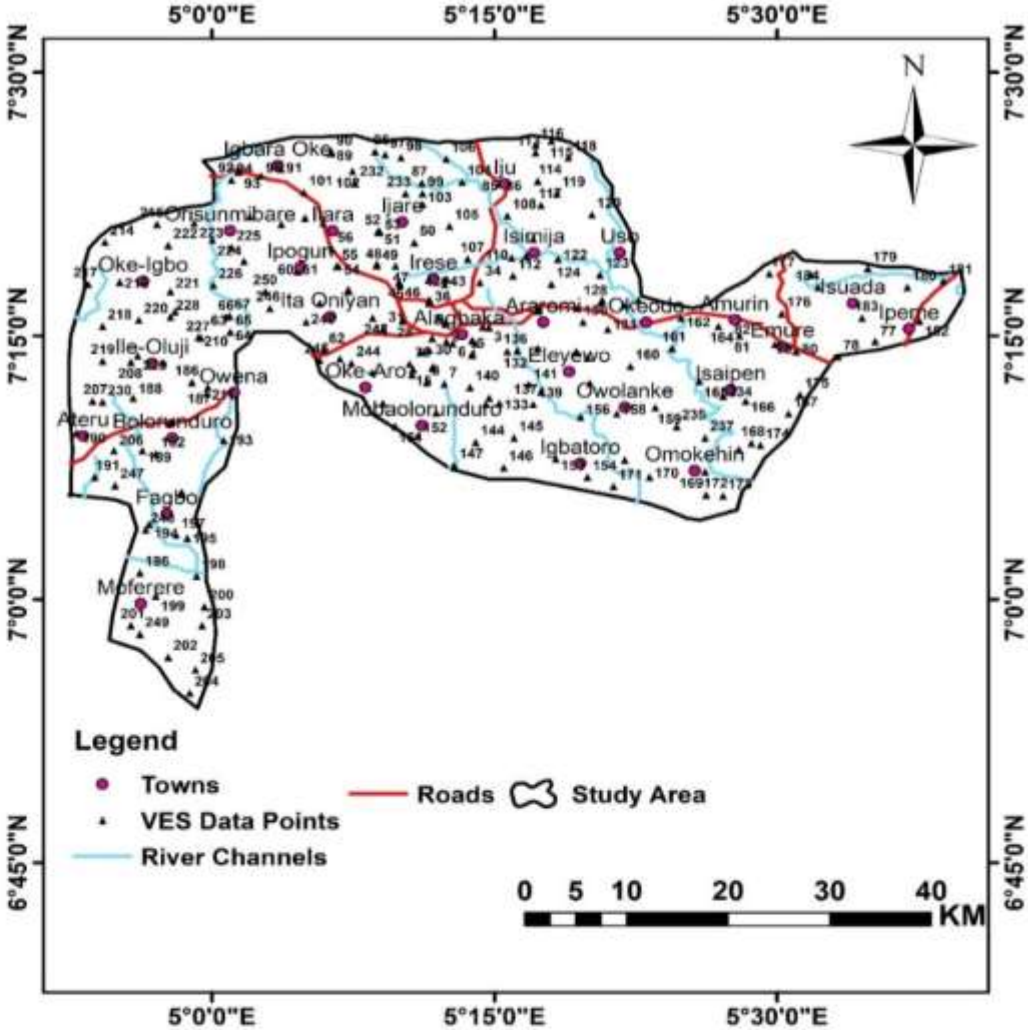

Fig. 3. VES data acquisition map of the study area

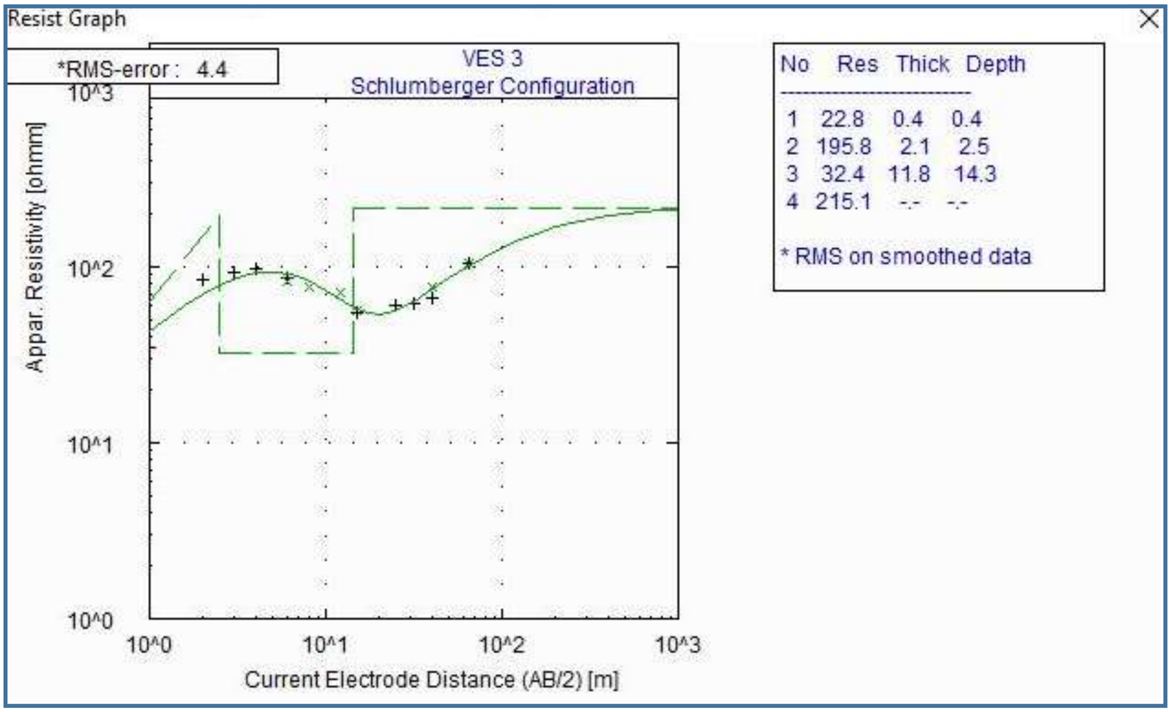

Fig.4a: KH Curve type delineated in the study area

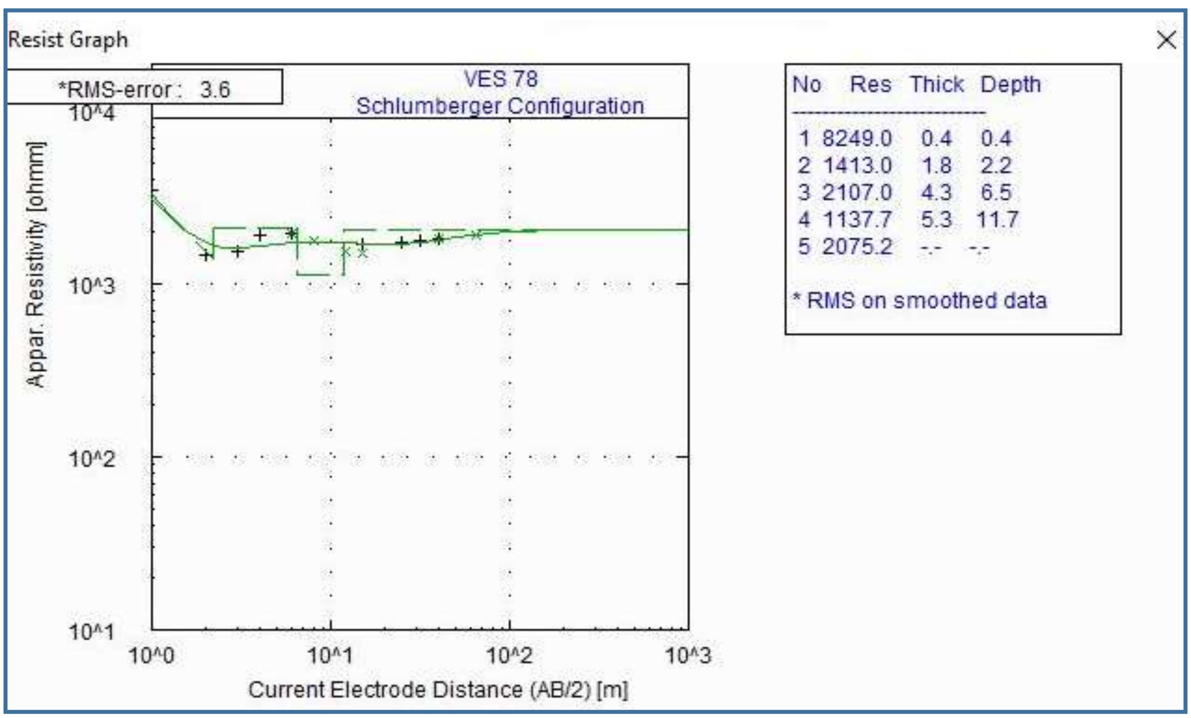

Fig.4b: HKH Curve type delineated in the study area

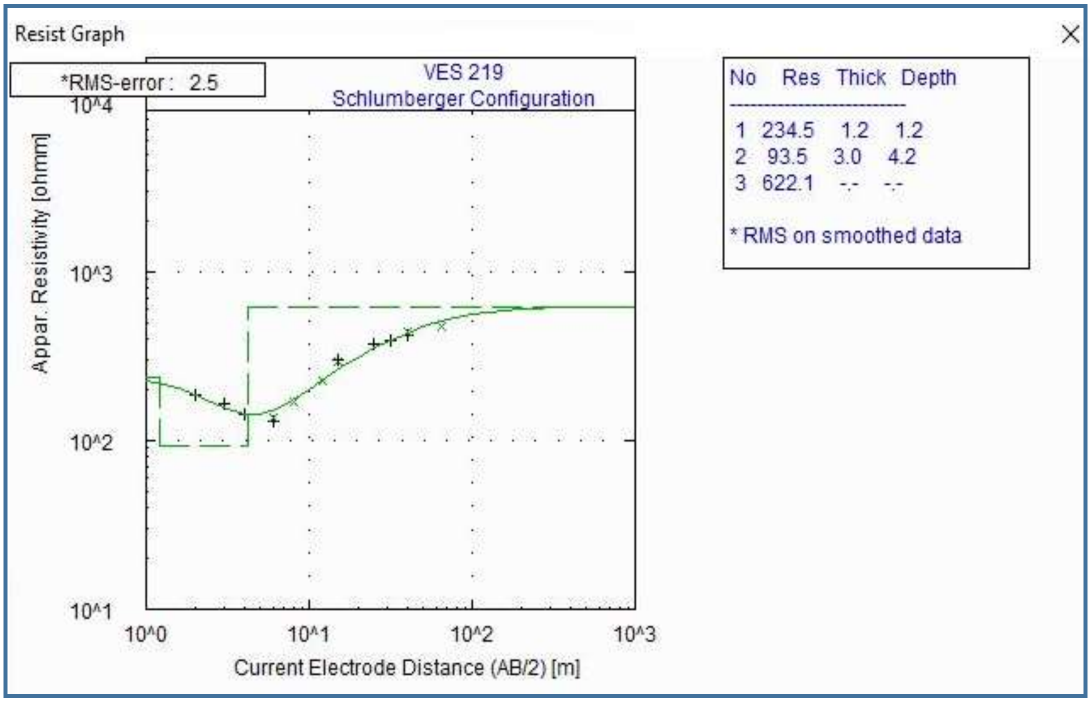

Fig.4c: H Curve type delineated in the study area

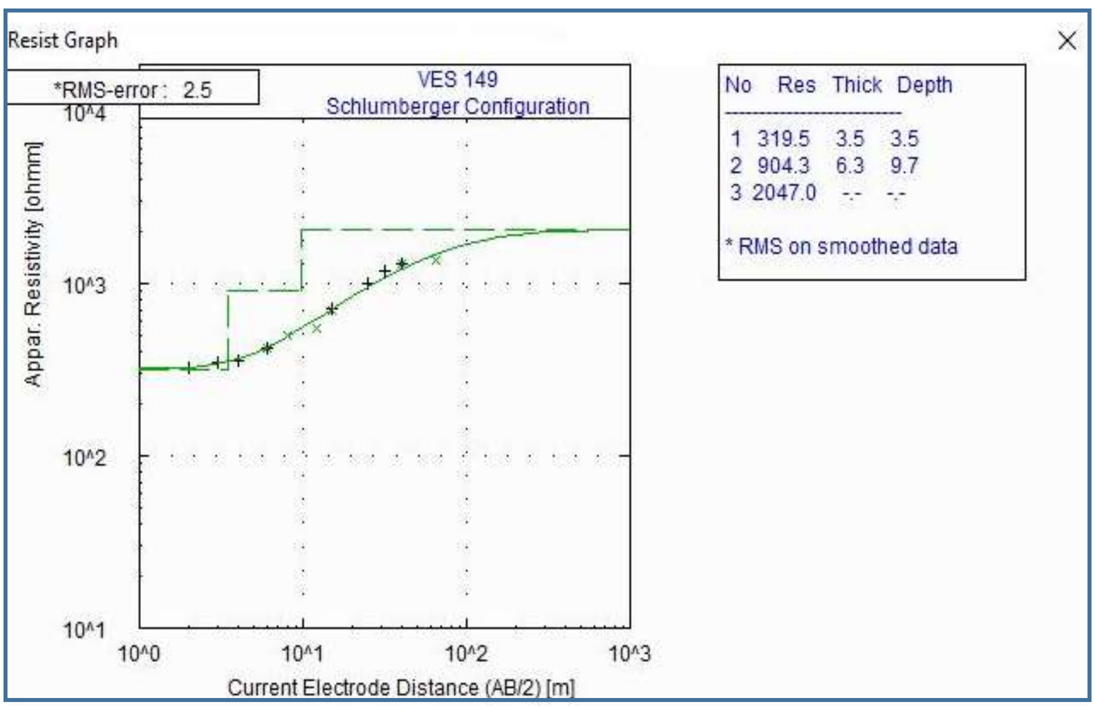

Fig.4D: A Curve type delineated in the study area

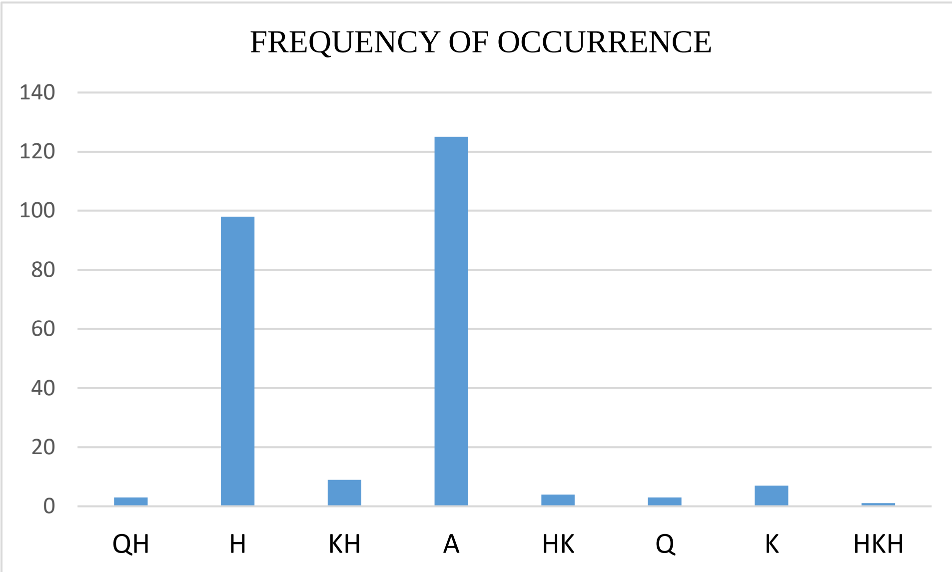

Table 2. Summary of interpreted geoelectric result from the VES data

VES no	Layer Resistivity (Ωm)	Layer thickness (m)	Curve Type	Infered geoelectric layers	Infered presence of aquifer layer
	$\rho_1/\ \rho_2/\ \rho_3/\ \rho_4/\ \rho_5$	$h_1/h_2/\ h_3/\ h_4$			
1	606/170/26/339	0.5/12.4/7.8	QH	Top soil/partially weathered layer/weathered layer/ basement	Present (Layer 3)
2	536/181/779	1.3/10.2	H	Top soil/weathered layer/basement	Present (Layer 2)
3	65/207/37/481	0.7/3/6.2	KH	Top soil/partially weathered layer/weathered layer/ basement	Present (Layer 3)
4	603/1245/2190	2.6/9	A	Top soil/weathered layer/fresh basement	Not present
5	114/54/815	2.1/6.6	H	Top soil/weathered layer/ fresh basement	Not present
.	.	.	.	.	.
.	.	.	.	.	.
50	10/222/394	0.6/9.9	A	Top soil/weathered basement/ basement	Not present
.	.	.	.	.	.
.	.	.	.	.	.

100	250/384/1510	2.2/11.1	A	Top soil/weathered basement/fresh basement	Present (Layer 2)
.	.	.	.	.	.
.	.	.	.	.	.
200	230/572/959	1.2/9	A	Top soil/weathered basement/basement	Not present
.	.	.	.	.	.
.	.	.	.	.	.
246	584/157/1775	1.3/7.7	H	Top soil/weathered basement/fresh basement	Present (Layer 2)
247	164/490/729	1.9/10.5	A	Top soil/weathered basement/ basement	Not present
248	69/526/815	1.6/7.8	A	Top soil/weathered basement/basement	Not present
249	509/188/491	2.2/9.7	H	Top soil/weathered basement/basement	Present (Layer 2)
250	358/193/751	2/10	H	Top soil/weathered basement/basement	Present (Layer 2)

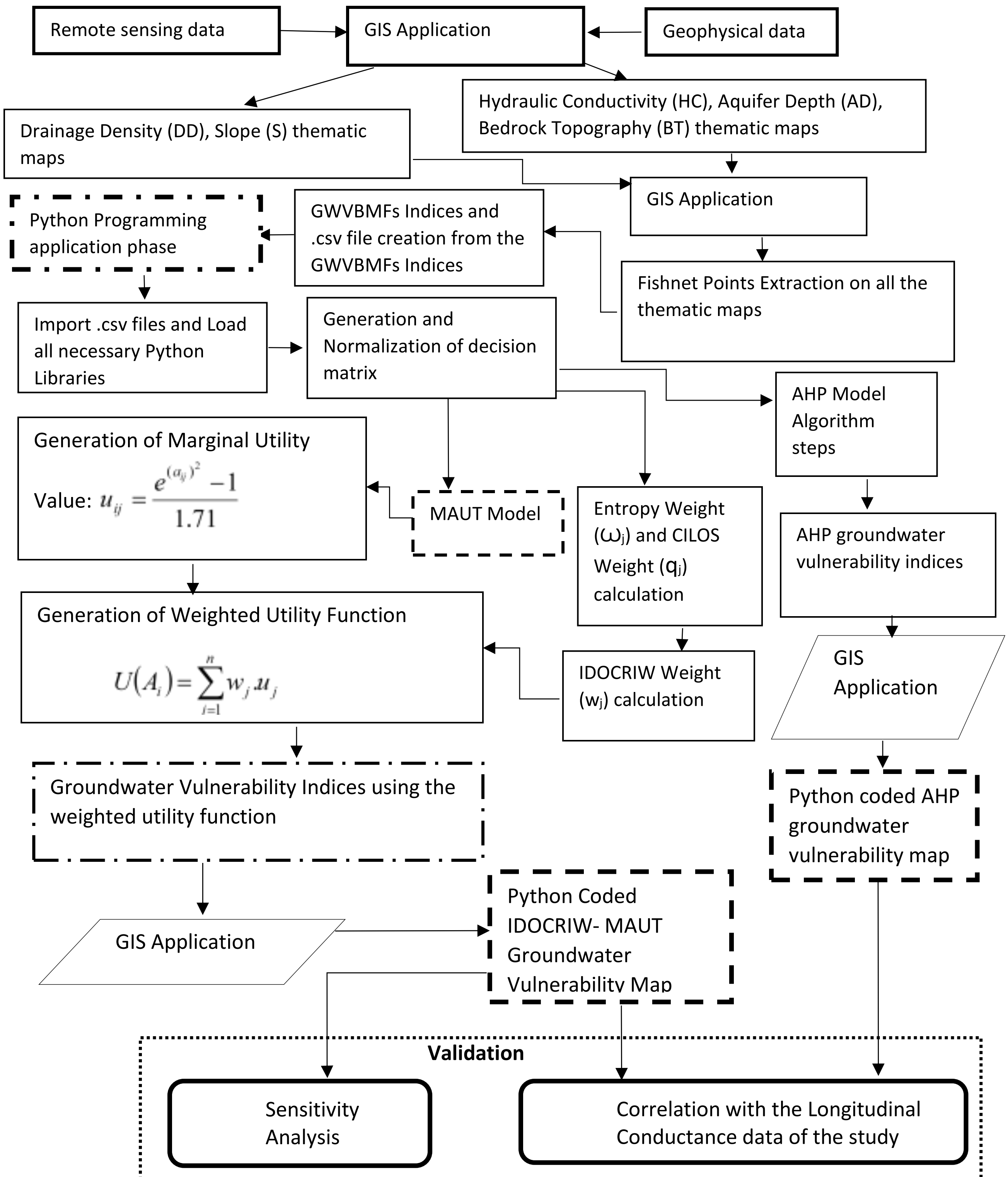

Fig. 6. Methodology flowchart for the groundwater vulnerability modelling

3.2. Methods

The diversity of data available in the research area determines how many thematic layers are used to evaluate GVMFs. Five theme layers were selected as the primary criterion for this investigation. Two forms of data were collected: remote sensing data, involving drainage density (DD) and slope (S), and traditional data, consisting of bedrock topography (BT), hydraulic conductivity (HC), and aquifer depth (AD). Comprehending the hydrological factors that affect the vulnerability of groundwater depends heavily on these determinants. They provide a strong foundation for a thorough assessment of the groundwater risk of an area. **Fig. 6** shows the full process of GVMF prediction. This study identified possible groundwater vulnerability sites using the MCDM technique. The theories and uses of the MCDM models used in this research were addressed in the proceeding subsections. These MCDMs comprise a variant ranking model for ranking alternative fishnet sites and an objective weighting model for generating the objective weight of the modelling components. These models include the integrated determination of objective criteria weights (IDOCRIW), which is used for objective weightage assignment; the multi-attribute utility theory (MAUT) model, which is used to rank the alternatives; and the analytical hierarchy process (AHP), which is used for comparative evaluation.

3.2.1. Integrated Determination of Objective Criteria Weights (IDOCIRW) model

Zavadskas and Podvezko introduced the IDOCRIW technique in 2016 (Trinkuniene et al., 2017). It uses the entropy weightage approach and criterion impact losses (CILOS) methodologies to calculate the objective weights of criteria. IDOCRIW considers in addition the relevance of the parameters selected, as well as the influence that the loss of the criteria selected can have on deciding the entire criteria weight, resulting in weight values that accurately combine the significance of the criteria with its loss impact to provide more plausible and effective weight values (Vinogradova et al., 2018; Zavadskas et al., 2017). Ayan et al. (2023) provided an in-depth examination of IDOCRIW, while multiple scholars (e.g., Alinezhad and Khalili, 2019; Alao et al., 2021) effectively implemented the IDOCRIW weighting method in a variety of fields of study, such as construction and renewable energy, and offered the benefits and drawbacks of IDOCRIW as an objective weighting technique.

The IDOCRIW algorithm procedures are provided in Eqs. 3 to 16:

Entropy weighting *processes are demonstrated from eqs. 3 to 7*

Step 1: Decision matrix of the criteria is formed as in eq. 3

$$X = \left(X_{ij}\right)_{mxn} = \begin{pmatrix} x_{11} & x_{12} & \cdots & x_{1n} \\ x_{21} & x_{22} & \cdots & x_{2n} \\ \vdots & \vdots & \cdots & \vdots \\ x_{1m} & x_{2m} & \cdots & x_{mn} \end{pmatrix}_{m\times n} \tag{3}$$

where 'X' is the matrix that defines the alternatives and criteria, 'Xim' are the potential alternatives, 'Xjn' are the assessment criteria, 'm' is the quantity of alternatives, and 'n' is the quantity of criteria to be evaluated.

Step 2: The decision matrix is normalized as in eq. 4

$$r_{ij} = \frac{x_{ij}}{\sum_{i=1}^{m} x_{ij}} \qquad i = 1, 2\ldots m; j = 1, 2\ldots n \tag{4}$$

Step 3: The degree of entropy is then calculated as in eq. 5

$$e_j = -\frac{1}{In(m)}\sum_{i=1}^{m} r_{ij}.In\left(r_{ij}\right) \qquad 0 \leq e_j \leq 12 \qquad i = 1, 2\ldots m; j = 1, 2\ldots n \tag{5}$$

Step 4: The degree of entropy divergence is gotten as in eq. 6

$$d_j = 1 - e_j \qquad j = 1, 2 \ldots n \tag{6}$$

Step 5: Entropy weight (w) is then calculated using eq. 7

$$w_j = \frac{d_j}{\sum_{i=1}^{m} d_j} \tag{7}$$

Note, $\sum_{j=1}^{m} w_j = 1$ j =1, 2 … m.

Processes for ***CILOS weighting*** *are demonstrated in Eqs. 8 to 15:*

As noted by Zavadskas and Podvezko (2016), decision matrix normalization as in eq. 4 is not a prerequisite in CILOS. However, normalizing the data helps to see the impact suffered by the criteria in the CILOS weighting model.

Step 6: After normalization has been performed, minimized criteria (non-beneficial) values are made beneficial leveraging on eq. 8 before the square matrix is produced employing eq. 9. However, if all criteria are beneficial, then we skip the step and go to the creation of the square matrix as given in eq. 9.

$$r_{ij} = \frac{\min_i r_{ij}}{r_{ij}} \tag{8}$$

$$A = \left\| a_{ij} \right\| \left(a_{ii} = r_{ii}; a_{ij} = r_{kjj} \right) \tag{9}$$

Step 7: The matrix of the relative loss P is then created as given in eq. 10 and eq. 11

$$p = \left\| p_{ij} \right\| \tag{10}$$

$$p_{ij} = \frac{r_j - a_{ij}}{r_j} = \frac{a_{ii} - a_{ij}}{a_{ii}} \tag{11}$$

Note: the diagonal elements of the matrix P are 0. The elements of p_{ij} in the matrix P give the relative loss of the jth criterion, if the ith criterion is selected as the best criteria.

Step 8: The matrix F is then determined as shown in eq. 12

$$F = \begin{bmatrix} -\sum_{i=1}^{m} p_{i1} & p_{12} & \cdots & p_{1m} \\ p_{21} & -\sum_{i=1}^{m} p_{i1} & \cdots & p_{2m} \\ \vdots & \vdots & \cdots & \vdots \\ p_{m1} & p_{m2} & \cdots & -\sum_{i=1}^{m} p_{i1} \end{bmatrix}_{n \times n} \tag{12}$$

Step 9: Then the weights (q_1, q_2 … q_m) of the criteria are obtained by solving the system of homogeneous linear equation given in eq. 13

$$F \times q_j = 0 \tag{13}$$

Step 10: The criteria weights q_j are the result of the system of the linear equation which can be solved using the method of Ali et al (2020). This is shown in eq. 14

$$q_j = F^{-1} z \tag{14}$$

Where z is a vector near 0 and to determine its value, it is assumed that its first element is closer to 0 while others are zero. Thereby, the form of vector z is highlighted in eq. 15;

$$Z = \begin{bmatrix} 0.000 & 0 & 0 & 0 & 0 & 0 & 0 & 0 & 0 & 0 & 0 & 0 & 0 & 0 \end{bmatrix}^T \tag{15}$$

The CILOS weight vector q_j is then normalized so that, $\sum_{j=1}^{m} q_j = 1$

IDOCRIW weight determining step

The IDOCRIW weight is then determined through the integration of the Entropy and CILOS weight gotten for the criteria. This integration method is shown in eq. 16

$$\omega_j = \frac{w_j . q_j}{\sum_{j=1}^{n} w_j . q_j} \tag{16}$$

However, it is to be noted that the higher the IDOCRIW weight of a criterion, the more significant/important it is. Python codes were used for the computation of the IDOCRIW weight of the vulnerability modelling factors.

3.2.2. Multi-Attribute Utility Theory (MAUT) Model

The MAUT model is centred on Von Neumann and Morgenstern's concept of utility from 1976, with the method's procedures extended subsequently by Keeney and Raiffa in 1983 (Emovon et al., 2016). Çetinkaya et al. (2023) recommend the MAUT model as the preferred MCDM technique based on its straightforward evaluation of alternative processes. It should be emphasized as well that, before using the MAUT model to rank the alternatives, the weights of the criterion must be calculated using one of the weight allocation models. Scholars (Adalı and Işık, 2017; Işık and Koşaroğlu, 2020) have used the MAUT model to make decisions across multiple fields, such as the societal economy and industrialization.

*The algorithm steps of **MAUT** are presented as follows*

Step 1: The decision matrix detailing the factors and the alternatives is determined as in eq. 17.

$$X = \begin{bmatrix} x_{11} & x_{1j} & \cdots & x_{1n} \\ x_{i1} & x_{ij} & \cdots & x_{in} \\ \vdots & \vdots & \cdots & \vdots \\ x_{m1} & x_{mj} & \cdots & x_{mn} \end{bmatrix}_{m \times n} \quad i = 1,2 \ldots m;\ j = 1,2 \ldots n \tag{17}$$

Step 2: The decision matrix is then normalized as in eq. 18 for the maximizing criteria and eq. 19 for the minimizing criteria

$$a_{ij}(x_{ij}) = \frac{x_{ij} - \min(x_{ij})}{\max(x_{ij}) - \min(x_{ij})} \qquad i = 1,2...m;\ j = 1,2...n \tag{18}$$

$$a_{ij}(x_{ij}) = 1 + \left(\frac{\min(x_{ij}) - x_{ij}}{\max(x_{ij}) - \min(x_{ij})} \right) \qquad i = 1,2...m;\ j = 1,2...n \tag{19}$$

Step 3: The marginal utility value (u_{ij}) of the *i*th alternative in terms of the *j*th criterion is determined using eq. 20

$$U(A_i) = \sum_{j=1}^{n} w_j.u_j \quad i = 1,2...m;\ j = 1,2...n \tag{20}$$

Step 4: The weighted utility function is then calculated as in eq. 21 and the higher the weighted utility, the better the alternative.

$$U(A_i) = \sum_{j=1}^{n} w_j.u_{ij} \tag{21}$$

3.2.3 The developed python based IDOCRIW-MAUT groundwater vulnerability model

As was determined in the previous section's numerical steps of the MAUT model, the weights of the criteria had to be determined with either the subjective or objective weight creation model in order to leverage the MAUT model to rank the alternatives. The basic concept behind the IDOCRIW–MAUT modelling algorithm is that, in order to eliminate expert opinion from the model during the computational process, the objective weight of the criteria was produced using the IDOCRIW model to prevent expert bias in the weighting. Albeit, three elaborate sections are involved in the generation of the IDCORIW. The **first** section showcases the generation of the entropy weight of the GWVBMFs, taking the initial decision matrix (**Table S1**) as input in the entropy algorithm steps to compute the entropy weight of the GWVBMFs. The **second** section deals with utilizing the initial decision matrix (**Table S1**) in the algorithm steps of CILOS to generate the weight system matrix (**Table 3**) needed to form the weight system matrix equation (eq. 22). The weight system matrix serves as an important parameter when employing the CILOS weighting model because it showcases the loss suffered by a criterion while assigning the best value to the other criteria. The solved weight system matrix employing Ali et al. (2021) approach offered the CILOS weight of the GWVBMFs.

Table 3. The weight system matrix of the GWVBMFs

SL	DD	HC	AD	BT
-2.51724138	0.64285714	0.33520337	0.80236486	0.00000000
0.93103448	-2.71428571	0.9898317	0.82094595	0.52107963
0.86206897	0.73809524	-2.28786816	0.75675676	0.25607852
0.72413793	0.69047190	0.62762973	-3.18243243	0.20231988
0.00000000	0.64285714	0.33520337	0.80236486	-0.97947803

$$\begin{pmatrix} -2.51724138 & 0.64285714 & 0.33520337 & 0.80236486 & 0.00000000 \\ 0.93103448 & -2.71428571 & 0.9898317 & 0.82094595 & 0.52107963 \\ 0.86206897 & 0.73809524 & -2.28786816 & 0.75675676 & 0.25607852 \\ 0.72413793 & 0.69047190 & 0.62762973 & -3.18243243 & 0.20231988 \\ 0.00000000 & 0.64285714 & 0.33520337 & 0.80236486 & -0.97947803 \end{pmatrix} \times q^T = 0 \qquad (22)$$

The third **section** is then the generation of the IDOCRIW weight from the integration of the entropy and CILOS weight already gotten. **Table 4** details the computed values of the IDOCRIW weight of the GWVBMFs.

Table 4. IDOCRIW weight of the GVMFs alongside the entropy and CILOS weight values

GWVBMFs	Entropy Weights (w_j)	CILOS Weight (q_j)	IDOCRIW weights (ω_j)
SL	0.375395	0.156528	**0.365249**
DD	0.126261	0.145165	**0.113930**
HC	0.366750	0.172221	**0.392613**
AD	0.116034	0.123811	**0.089300**
BT	0.015560	0.402275	**0.038908**

The computed weights were then incorporated into the MAUT algorithm process to form the IDOCRIW-MAUT model used for ranking the alternative fishnet points according to their susceptibility threat to produce the area's groundwater vulnerability index (GWVBI) (**Table S2**) of the study area. This extensive methodology, together with the computational processes performed using Python program (Appendix A1 – A5), provides a reliable method for building a groundwater vulnerability model index required for making innovative threat assessments of the study area.

3.2.3. Analytical hierarchical process (AHP) model

Saaty introduced the AHP model in 1980 to evaluate numerous decision-making processes and determine the subjective weight of the criterion. (Saaty, 1994; Saaty and Ozdemir, 2021). The AHP is a complex decision-making process that organizes an arduous issue into a hierarchy, breaking down concerns into levels that comprise goals, variables, and choices, which are subsequently assessed both instinctively and analytically (Ozegin et al., 2023, 2024a). In the AHP model, a pairwise comparison matrix and normalized principal eigenvectors are used to calculate the subjective weights of criteria with equivalent judgment scores. 'Saaty's scale of relevance' is commonly used to calculate the judgment scores required to create a pairwise comparison matrix (**Table 5**).

Table 5. Saaty scale of relevance

Verbal judgment of relevance	Numerical rating
Equal relevance	1
Equal to moderate relevance	2
Moderate relevance	3
Moderate to strong relevance	4
Strong relevance	5
Strong to very strong relevance	6
Very strong relevance	7

Very strong to extreme relevance	8
Extreme relevance	9

Furthermore, Kumar et al. (2022) believe that the two terms 'consistency index' and 'consistency ratio' established by Saaty are aimed at verifying the uniformity and dependability of the created AHP weights so that if the weights do not meet the consistency conditions, the pairwise comparison can be modified to obtain acceptable weights. The methodical procedure for using the AHP model is detailed in the subsequent steps:

Step 1: The hierarchical framework for the pairwise comparison of parameters is being developed. Eq. 23 applies to calculate the entirety of comparisons that will be made using opinions from experts.

Number of comparisons = $\frac{n(n-1)}{2}$, '*n*' is the number of criteria being considered (23)

Step 2: The normalized consolidated pairwise comparison is being determined employing geometric mean approach on the participants' comparison matrix as in eq. 24.

$$a_{ij}^{c} = \left(\prod_{k=1}^{n} a_{ij}^{k}\right)^{1/n} \tag{24}$$

Where, a_{ij}^{c} - consolidated pairwise comparison, a_{ij}^{k} - is the pairwise comparison given by participant, $\prod_{k=1}^{n}$ - product of the participants' inputs, *n* – is the number of participants, *1/n* – is the square root based on the number of participants.

Step 3: In order to generate the AHP weight, the largest eigenvalue (λ_{max}) is first calculated and the system of equation given in eq. 25 is then solved.

$$w_i = \frac{1}{\lambda_{maks}} \sum_{j=1} a_{ij} w_{ij} \text{ , } i = 1, 2,.., n \tag{25}$$

The generated weight is normalized such that $\sum_{i=1}^{n} w_i = 1$

Step 4: The generated weight is checked for consistency as in eq. 26

$$CR = \frac{CI}{RI} \tag{26}$$

where, CR is the consistency ratio and for consistent and acceptable AHP weights, CR must be < 0.1, CI is the consistency index given by, $CI = \frac{\lambda_{max}-n}{n-1}$, RI is the random index (**Table 6**) as given by Saaty (1987).

Table 6. Random index according to Saaty (1987)

Number of factors considered (n)	**1**	**2**	**3**	**4**	**5**	**6**	**7**	**8**	**9**	**10**
RI	**0**	**0**	**0.58**	**0.9**	**1.12**	**1.24**	**1.32**	**1.41**	**1.45**	**1.49**

The CR, which was determined to be less than 0.1 and calculated to be 0.0964, demonstrated that the weights obtained were consistent (**Table 7**).

Table 7. Consistency calculation

λ_{max}	n	RI	CL	CR	Reliability
5.43174	5	1.12	0.10793	0.0964	Less than 0.1

3.2.3.1 The AHP based groundwater vulnerability model

The groundwater vulnerability model in accordance with the AHP model is developed by using the resulting AHP criteria weight as well as the criteria ratings predicated on the location of each fishnet point according to the criteria's minimum or maximum direction. The AHP-based groundwater vulnerability indices (AHP-GWVBI) are then calculated using Python programs that modify the approach of Mogaji and Lim (2017), as shown in eq. 26.

$$AHP - GWVBI = Sl_{\omega} \times Sl_r + DD_{\omega} \times DD_r + HC_{\omega} \times HC_r + AD_w \times AD_r +. BT_w \times BT_r \quad (26)$$

A pairwise assessment matrix was utilized for comparing influencing factors (**Table 8**). The inverse values of the source array are subsequently incorporated into the base triangular array. The normalized quantities of the eigenvectors indicate the final indicator priority, and they are related to the proportional (ratio) matrix's maximum eigenvalues. The approach described here is the most effective way to reduce the effects of ratio inequalities. **Table 9** shows the appropriate values for the metrics. The overall technique produces proportionate weights, which are subsequently determined (**Table 10**). The Python codes (Appendix B) employed ensured a seamless computational process for the generation of the AHP weights.

Table 8. The matrix of pairwise comparisons

	SL	DD	HC	AD	BT
SL	1	2	0.5	3	1
DD	0.5	1	0.333	0.25	0.5
HC	2	3	1	4	2
AD	0.333	4	0.25	1	0.333
BT	1	2	0.5	3	1

Table 9. Matrix normalization

	SL	DD	HC	AD	BT
SL	0.203391	0.231919	0.204998	0.214632	0.203391
DD	0.091514	0.059455	0.086365	0.090183	0.091514
HC	0.359342	0.356799	0.351436	0.387271	0.359342
AD	0.142362	0.119908	0.152202	0.093281	0.142362
BT	0.203391	0.231919	0.204998	0.214632	0.203391

Table 10. Parameters determining the mapping of groundwater vulnerability and their AHP weights

Modelling factors	Feature/ Class	Unit	Area Covered (Km^2)	Percentage of Study Area Covered (%)	Rank	Normalized AHP Weight (W)	Modelling Direction on Groundwater Vulnerability
Slope	0 – 2		840	45	1	0.21167	Very low
	2 – 8		691	37	2		Low
	8 – 15	Degree (º)	261	14	3		Medium
	15 – 30		56	3	4		Medium high
	30 - 60		19	1	5		High
	Total		**1867**	**100**			
Drainage density	0.5 – 1.4		504	27	1	0.08381	Very low
	1.4 – 2.0		504	27	2		Low
	2.0 – 2.7	Km/Km^2	411	22	3		Medium
	2.7 – 3.5		317	17	4		Medium high
	3.5 – 5.2		131	7	5		High
	Total		**1867**	**100**			
Hydraulic conductivity	0 – 0.00391		149	8	5	0.36284	Very low
	0.00391 – 0.00830		299	16	4		Low
	0.00830 – 0.01301	m/day	392	21	3		Medium
	0.01301 – 0.01837		486	26	2		Medium high
	0.01837 – 0.04144		541	29	1		High
	Total		**1867**	**100**			
Aquifer depth	0 – 1.0		560	30	1	0.13002	Very low
	1.0 – 1.75		692	37	2		Low
	1.75 – 2.84	m	429	23	3		Medium
	2.84 – 5.00		149	8	4		Medium high
	5.00 – 12.72		3	2	5		High
	Total		**1867**	**100**			
Bedrock topography	166.5 – 239.3		188	10	1	0.21167	Very low
	239.3 – 312.1	m	429	23	2		Low

312.1 – 385.1	672	36	3	Medium
385.1 – 457.8	429	23	4	Medium high
457.8 – 530.6	149	8	5	High
Total	**1867**	**100**		

3.3 Fishnet Creation

Fishnets are built using geographic information system (GIS) software to build grids of regularly spaced cells for effective geospatial modelling in the study area (Frye et al., 2018). Uniformly arranged fishnet spots (**Fig. 7**) were placed on the theme layers in order to obtain pixel values from each point for reliable computations. As a result, for coordinated geospatial modelling, 175 fishnet points were constructed across the whole study region using the ArcGIS 10.7 data management tool's create fishnet point feature. These 175 fishnet points were then used to extract the GVMF's parameters from thematic maps, which will be reported in the results part of this study. The data frame containing the retrieved parameters was used as the modelling input in this study.

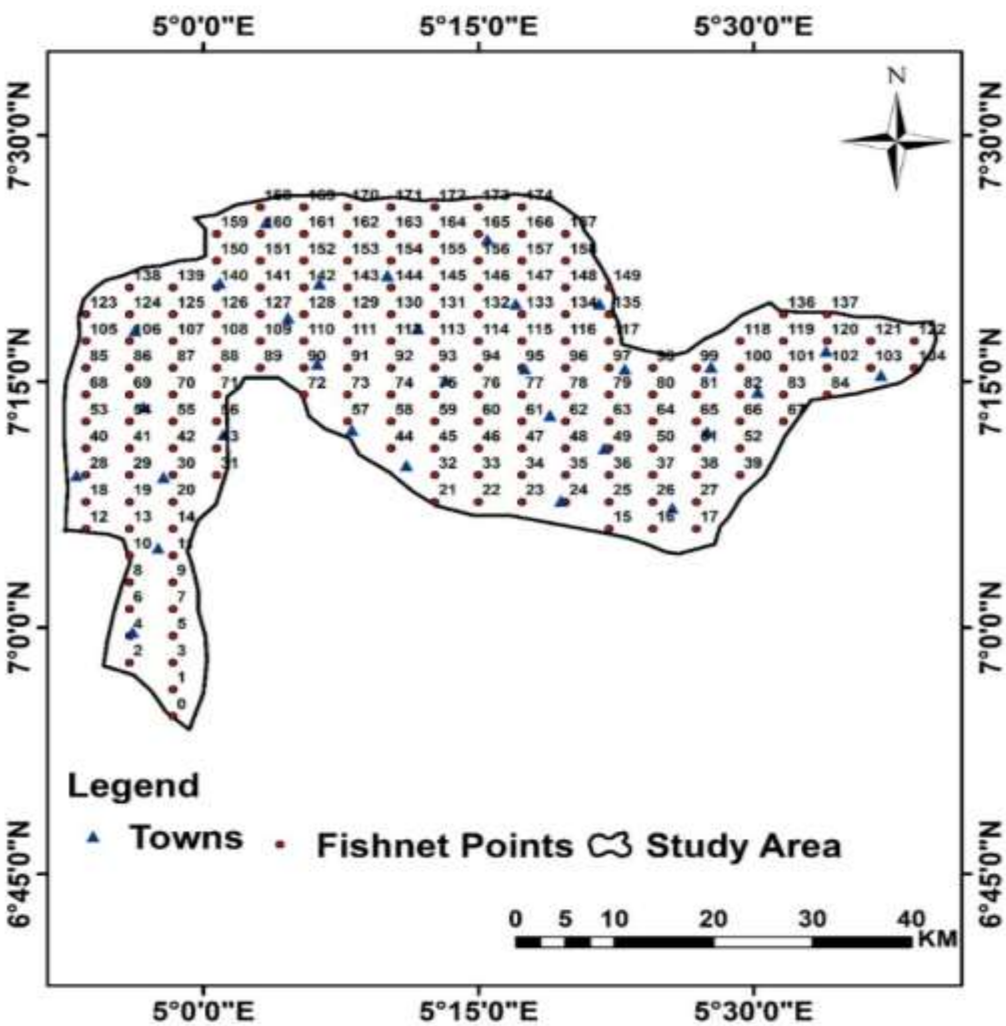

Fig. 7. Fishnet template map of the study area

3.4 Methods of model validation

3.4.1 Sensitivity analysis (SA)

SA is a tool for examining the adaptability of MCDM models to varied weight adjustments, as the weight allocated to criteria is a critical determinant that determines the model's ranking of alternatives. According to the perspectives of multiple scholars (Demir et al., 2024; Alao et al., 2021), a specific method for carrying out SA involves adjusting the weight of the highest weighted criteria over some chosen percentages, subsequently creating accompanying appropriate weights of the other criteria at this distinct weight of the initial highest weighted criteria, and ultimately creating different alternative ranking (in this vulnerability index) scenarios centred on the newly generated weights. The scenario outcomes can then be shown using a suitable visualization tool, such as a radar chart, heatmap, and others. In this instance, a heatmap of the VI's variability changes among the scenarios based on the study area's alternatives (i.e., fishnet points) was used. According to Kopp et al. (2014), an effective model will have minimal variability, while a less effective model will exhibit more variety in the heatmap.

3.4.2 Correlation with longitudinal conductance (LC) data

To evaluate the reliability and effectiveness of the IDOCRIW-MAUT groundwater vulnerability model, qualitative verification was performed by correlating the output indices with geophysical parameter (longitudinal conductance (LC)) data from the study area. As observed by different scholars (e.g., Tijani et al., 2021; Alao et al., 2022), considering LC assesses the aquifer's protective capacity, it can be used to qualitatively assess the efficacy of the created groundwater vulnerability model. In the present approach, the model's predicted groundwater vulnerability zones that inversely coincide with the interpreted LC data of that particular area are recognized as 'correlate,' while those that do not coincide are termed as 'not correlate.' According to equation (27), the correlated data will be utilized to calculate the % correlation/agreement between the model's prediction and the LC data.

$$PA = \frac{NCP}{NOB} \times 100\% \tag{27}$$

Where;

'PA' is the percentage agreement, 'NCP' is the number of correlation points, and 'NOB' is the number of observed points.

4. Results and Discussion

4.1. Groundwater vulnerability modelling factors (GWVBMFs)

For the groundwater risk modelling in this research, five (5) GWVBMFs were chosen from remote sensing and geophysical datasets, as mentioned in the preceding section. These GWVBMFs include bedrock topography (BT), hydraulic conductivity (HC), aquifer depth (AD), drainage density (DD), and slope (S). The following is a brief overview of the hydrogeological evaluation of these GWVBMFs:

4.1.1. Drainage Density (DD)

DD measures how common or densely packed drainage features (such as rivers and streams) are in a certain area (Tolche, 2021; Ozegin et al., 2023). In essence, it relates to the entire length of streams and rivers per unit area, which is commonly measured in kilometres per square kilometre (km/km²). The study region was divided into five subgroups: 0.5–1.4, 1.4–2.0, 2.0–2.7, 2.7–3.5, and 3.5–5.2 km/km² (**Fig. 8**). In GWVB evaluations, high DD indicates a higher potential for runoff and thus less penetration of contaminants into the subsurface, lowering the GWVB to contamination in that area, whereas low DD indicates a higher vulnerability to contamination (Thomas and Duraisamy, 2018). 448 km (24%) of the research area is covered by DD, which is medium-high to high.

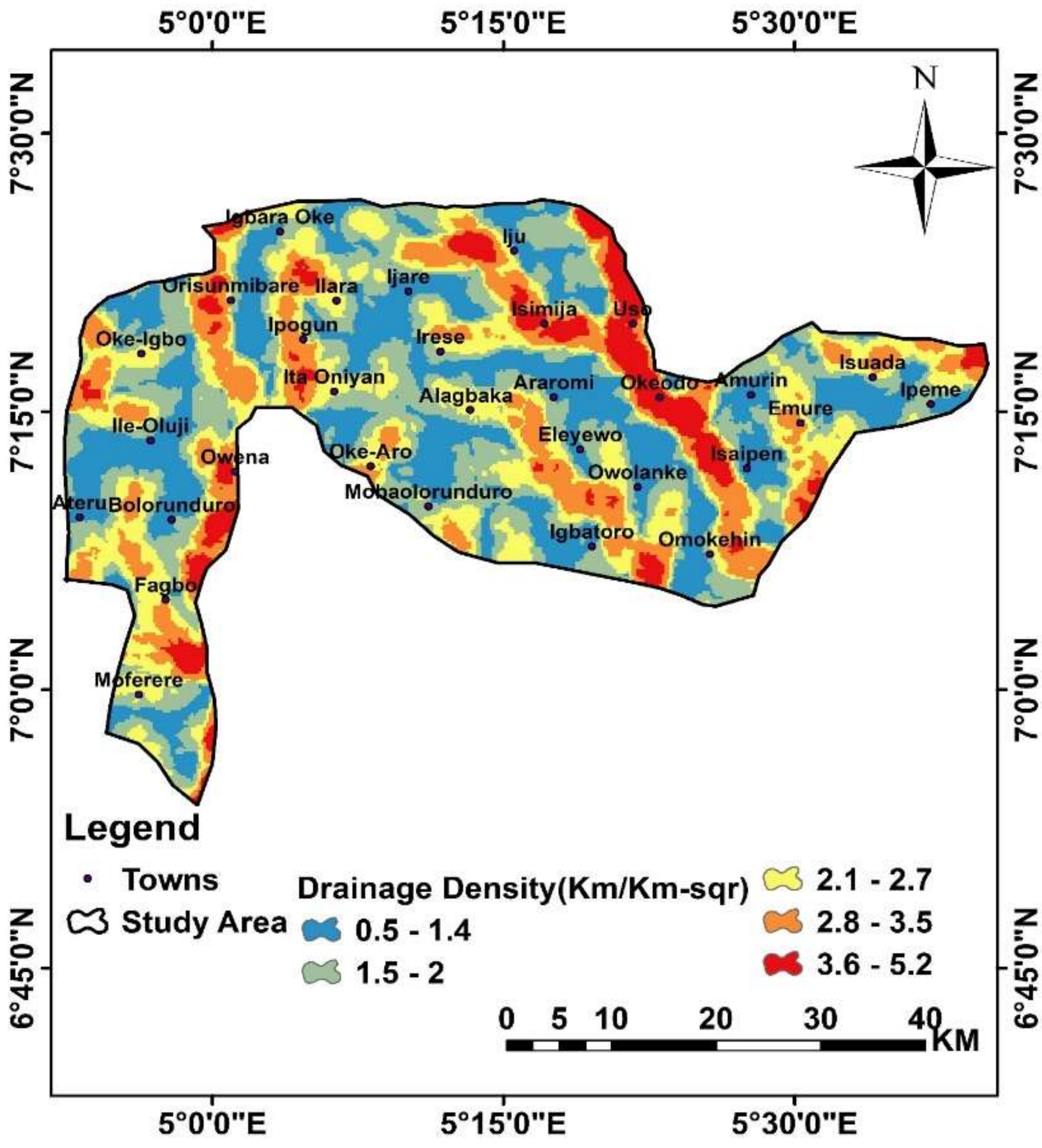

Fig. 8a. Drainage density of the study area

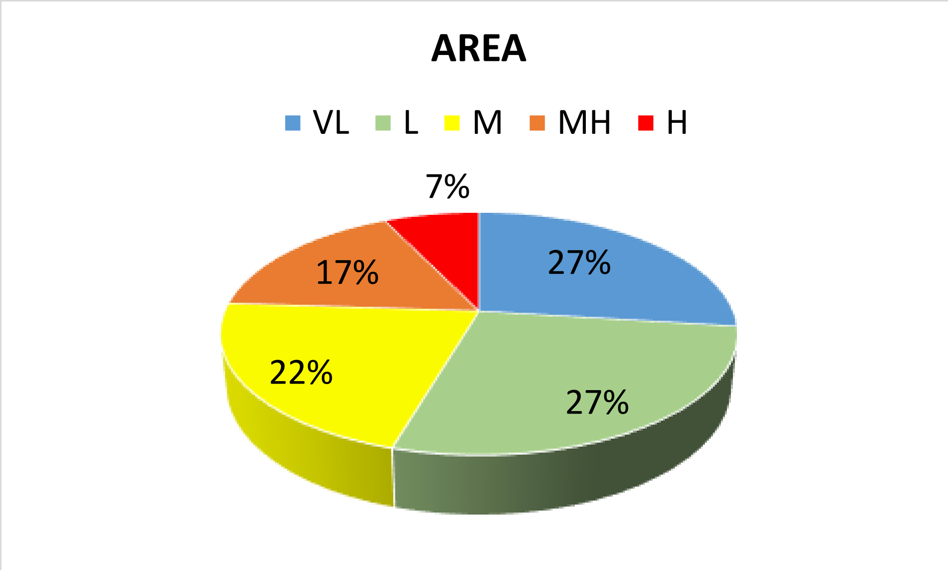

Fig. 8(b): Pie chart showing area coverage of each of the DD classes

4.1.2. Slope (S)

The Earth's surface inclination is measured by slope (S), which causes variations in surface water infiltration levels across different regions (Şener et al., 2018; Ozegin et al., 2024c). Typically, it is stated as a percentage or ratio of the elevation's ascent to its run. Slope regulates pollutant infiltration and discharge in the context of groundwater vulnerability assessment. As a result, areas with greater slopes will see more runoff and less pollutant infiltration, which will ultimately lessen the susceptibility of the groundwater in such areas and vice versa (Abu-Bakr, 2020). The values for the slope in the research area span from zero to sixty percent (**Fig. 9**). The values are reclassified into five groups: 0-2%, 2-8%, 8-15%, 15-30%, and 30-60%. The highest elevations, such as 15–30% and 30–60%, allow for a high level of runoff magnitude, which reduces the chance of potential cross-contamination. Three percent of these are found in the northern portion of the research area.

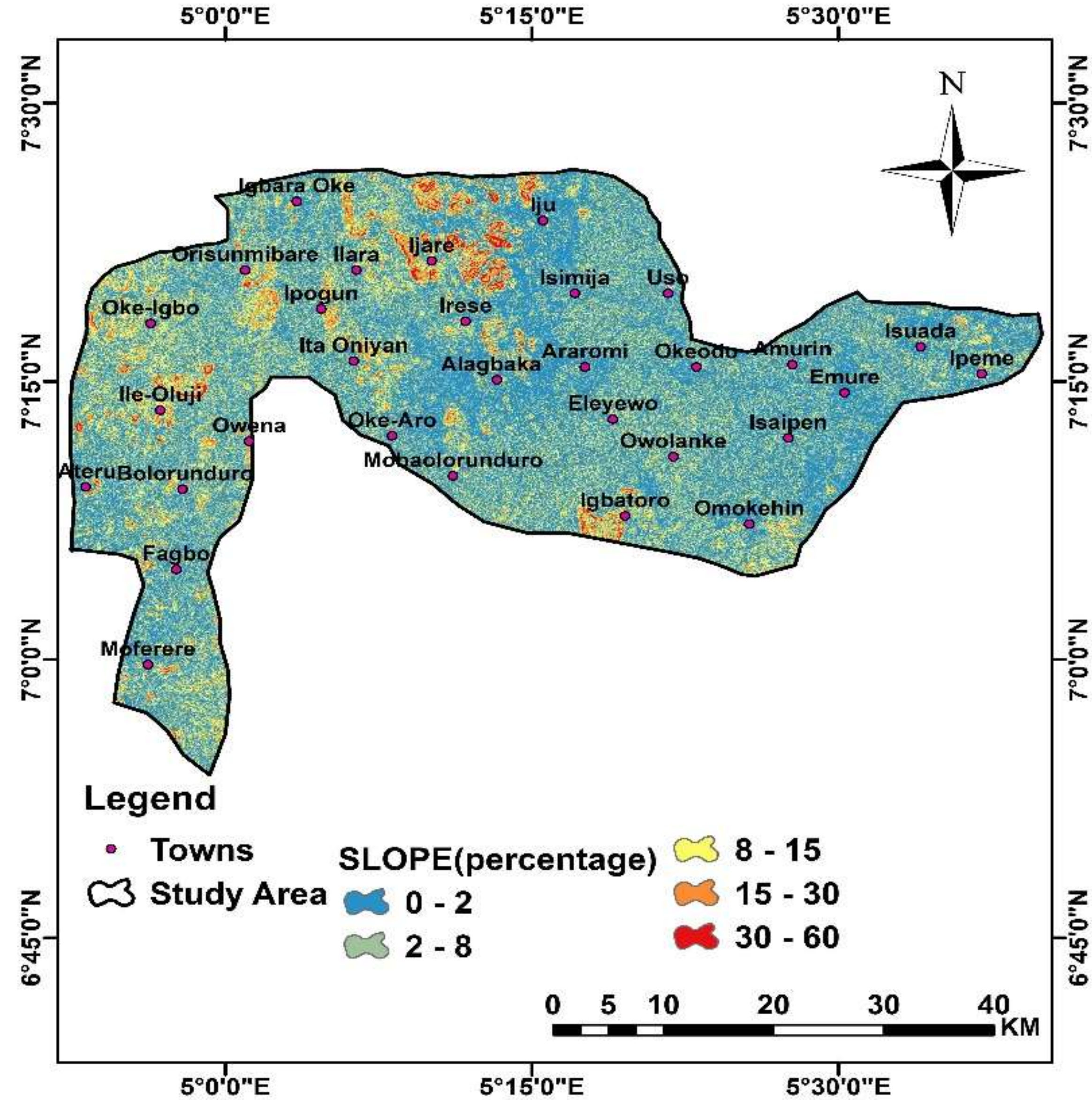

Fig. 9a. Slope map of the study area

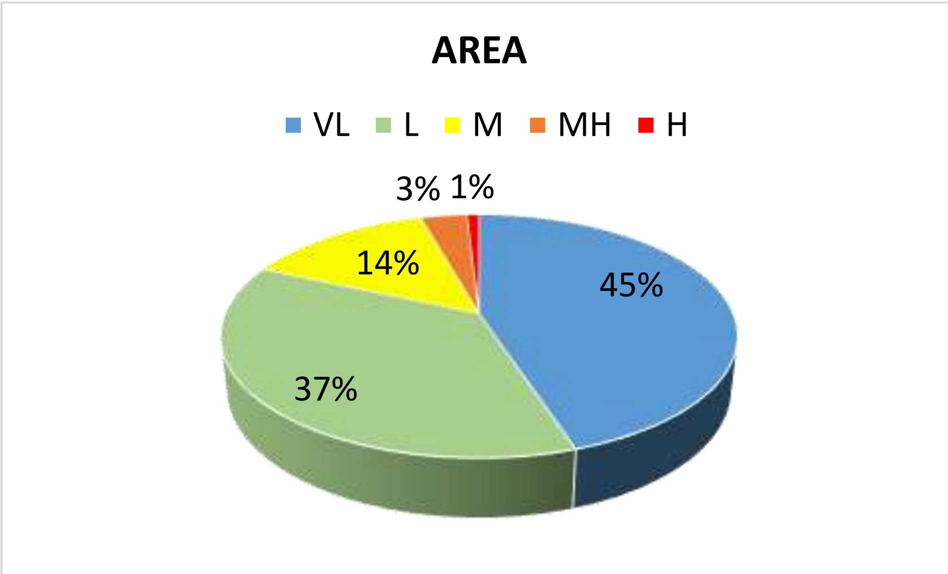

Fig. 9(b): Pie chart showing area coverage of each of the Slope classes

4.1.3 Aquifer Depth (AD)

The vertical distance between the topsoil and the top of the aquifer layer is known as the "aquifer depth" (AD) (Huan et al., 2020). The analysis of VES data from electrical resistivity data acquisitions yielded AD, a first-order geo-electric component. The study region was divided into five subgroups: 0–1.00, 1–1.00, 1.75–2.48, 2.48–5.00, and 5.00–12.72 (**Fig. 10**). According to the groundwater vulnerability study, regions with shallower aquifer depths are thought to be more prone to pollution, whereas regions with deeper aquifer depths are thought to be less susceptible to contamination (Ozegin et al., 2024b). In locations with deeper aquifer depths, pollutants travel greater distances, which causes them to be naturally filtered and weakened before they reach the groundwater network. In contrast, pollutants in regions with shallower aquifer depths traverse less, which means that less natural filtration takes place on them prior to their reaching the aquifer system (Rajput et al., 2020). Just 2% of the research is located in an aquifer that is comparatively deeper (5.00-12.72 m). This indicates that the research area's groundwater composition is extremely vulnerable.

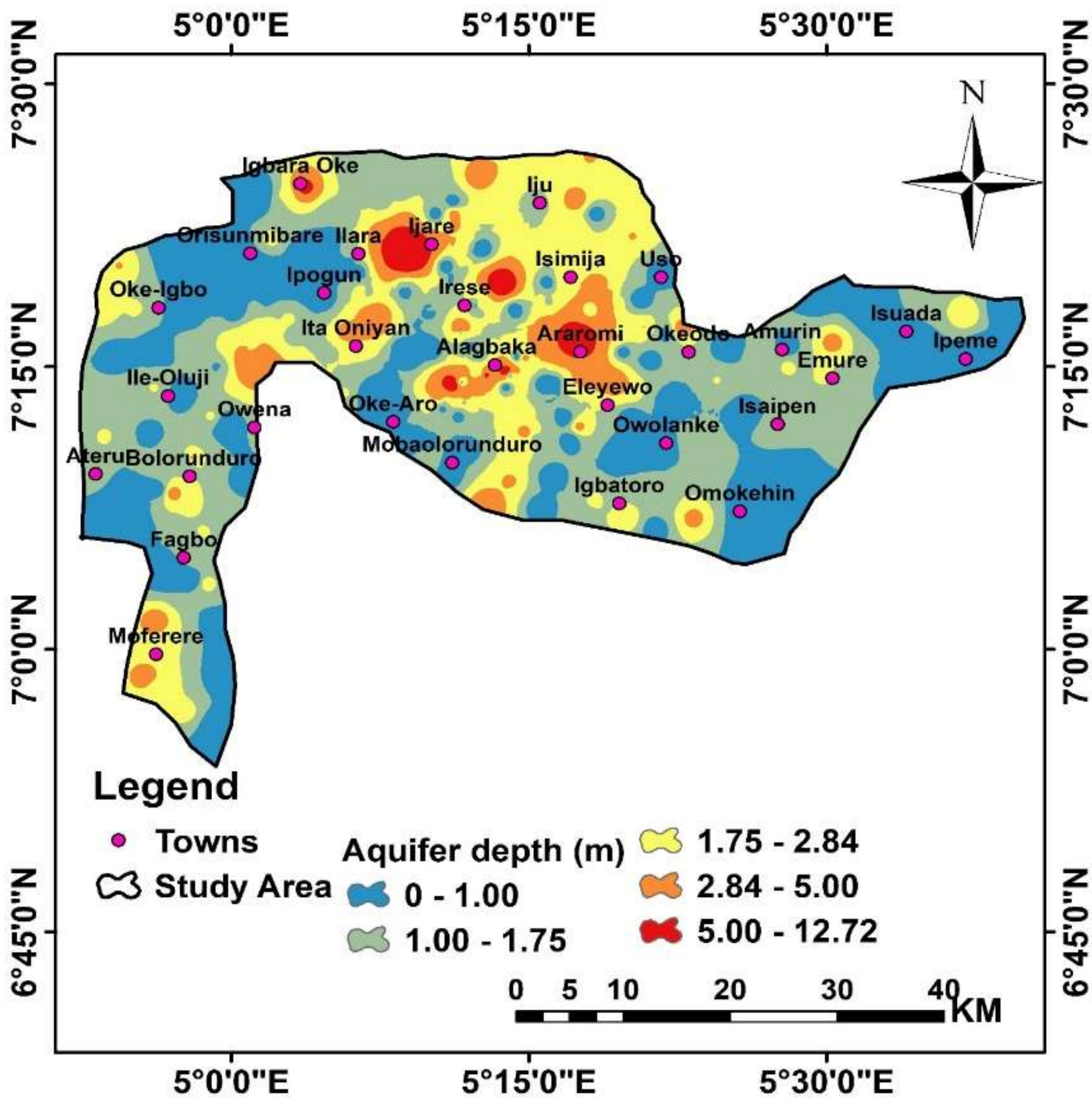

Fig. 10a. Aquifer depth map of the study area

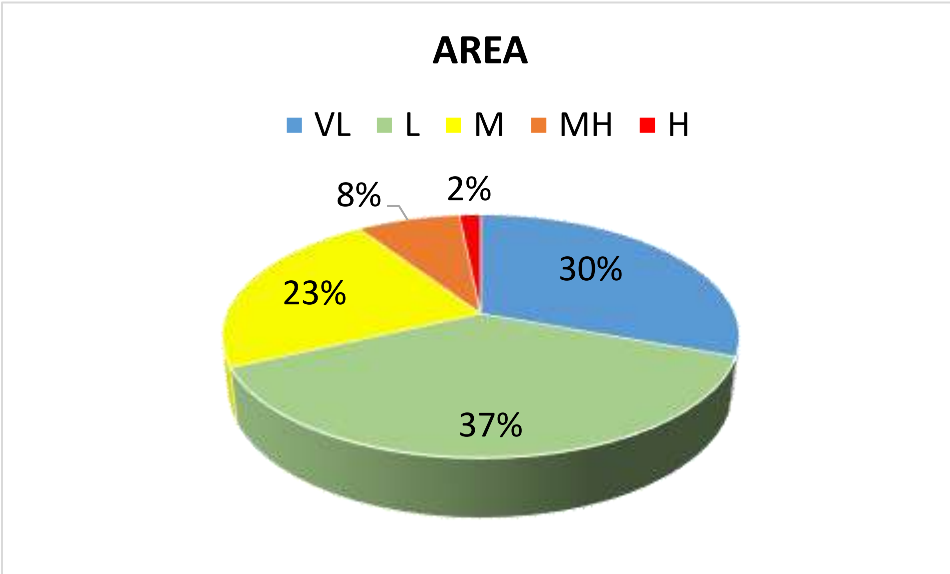

Fig. 10(b): Pie chart showing area coverage of each of the aquifer depth classes

4.1.4. Hydraulic Conductivity (HC)

The rate at which fluid (e.g., water) moves down a unit area of an aquifer under a unit hydraulic gradient is known as hydraulic conductivity (HC). This basically indicates how easily a fluid will flow through an aquiferous media (Akintorinwa et al., 2020; Gernez et al., 2019). The vertical electrical sounding (VES) data acquired by geophysical data capture can be interpreted to identify HC, a second-order geo-electric parameter. **Fig. 11** depicts the hydraulic conductivity (HC) variation throughout the research area. The aquifer HC fluctuates between 0 and 0.04144 m/day. In the study area, pollution of groundwater aquifers with high hydraulic conductivity ranged from 0.01837 to 0.04144 m/day representing 29% of the total area. Pollutant infiltration rises when HC readings or rankings are high (e.g., Fannakh and Farsang, 2022; Ozegin et al., 2024b). In broad terms, HC diminishes with increasing particle size. In addition to particle dimensions, the symmetry of the particles and their placement in the packing both have an impact on HC (Ozegin et al., 2024b).

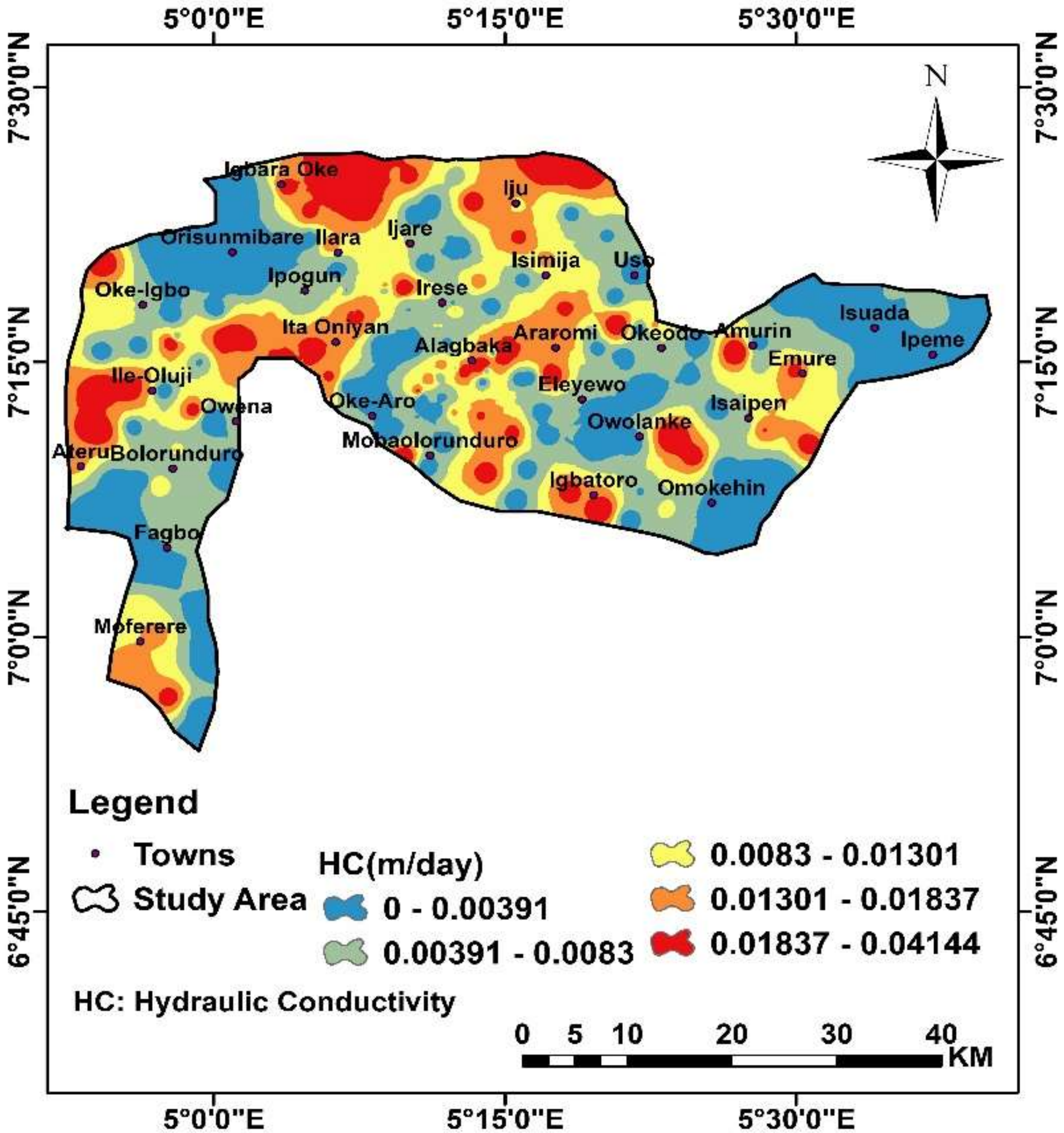

Fig. 11. Hydraulic conductivity map of the study area

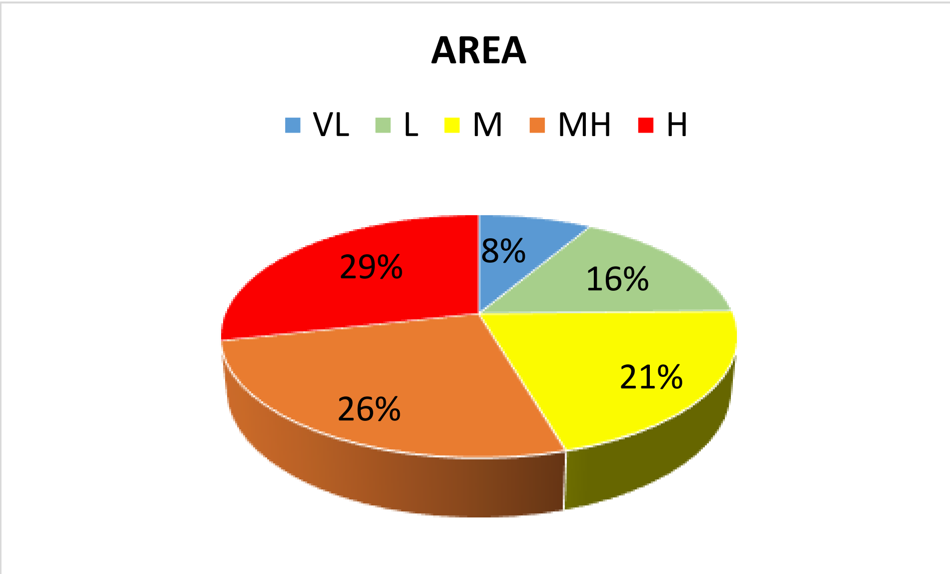

Fig. 11(b): Pie chart showing area coverage of each of the HC classes

4.1.5. Bedrock Topography (BT)

Bedrock topography (BT) refers to the altitude of a location's upper layer of bedrock. In basic terms, it represents how the bedrock appears if all of the overburden components were removed and observed from the top (Wells et al., 2020; Kellogg et al., 2017). BT values were determined from the analysis of VES data because depth to bedrock, which is critical for BT computation, can be derived from the VES data interpretation adopting Atenidegbe and Mogaji's (2023) technique. The study area was separated into five subsections: 166.5-239.3, 239.3-312.1, 312.1-385.1, 385.1-457.8, and 457.8-530.6 metres (**Fig. 12**). In terms of assessing groundwater vulnerability, regions with steep bedrock topography will witness pollutants remaining on them for a shorter period of time, which will reduce the volume of contaminants that reach the deeper aquifer units and, eventually, minimize vulnerability; on the other hand, areas with gentle bedrock will have pollutants remain on them for a longer period of time, which will result in higher vulnerability of groundwater (Olaseeni et al., 2021).

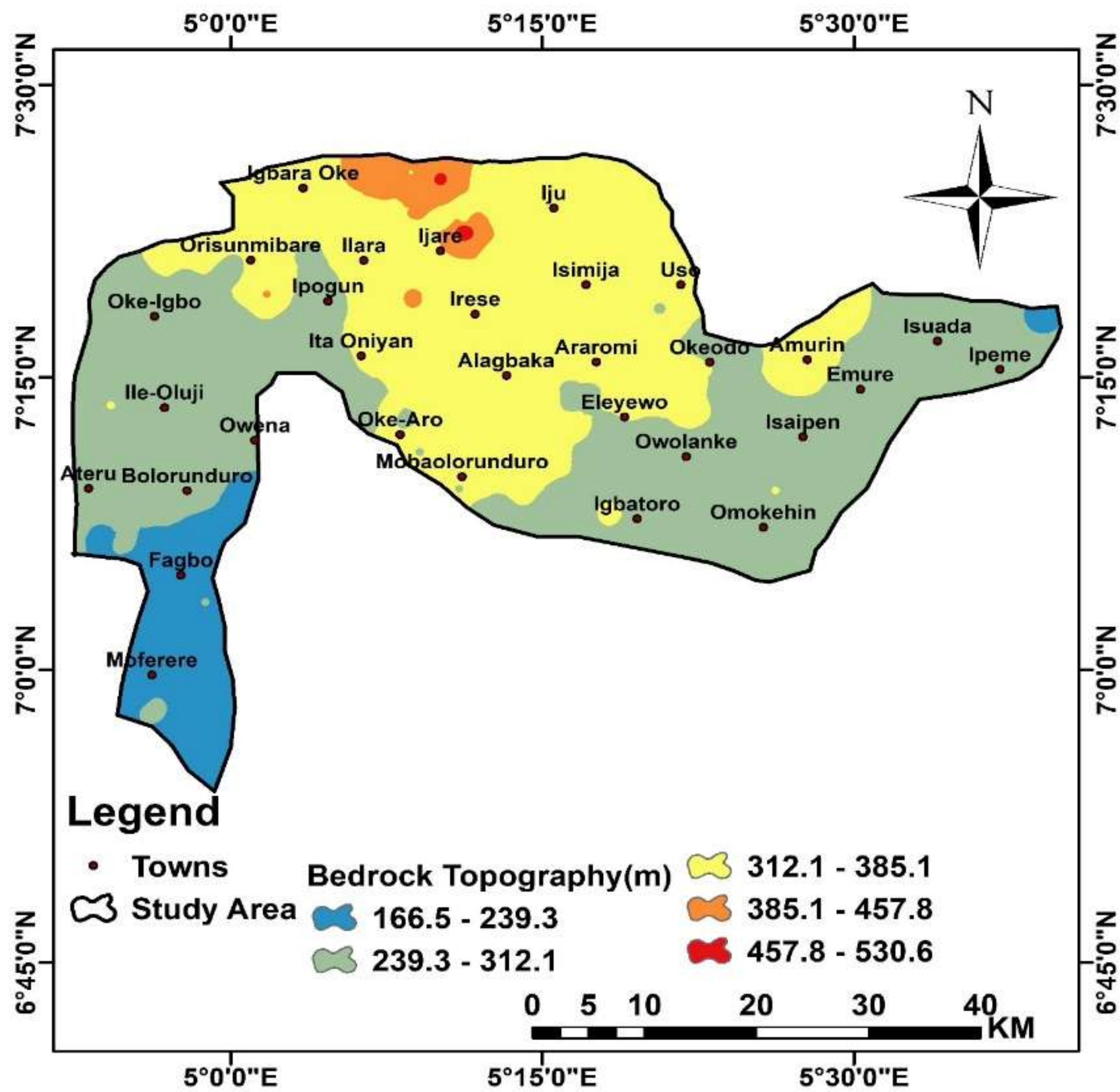

Fig. 12. Bedrock topography map of the study area

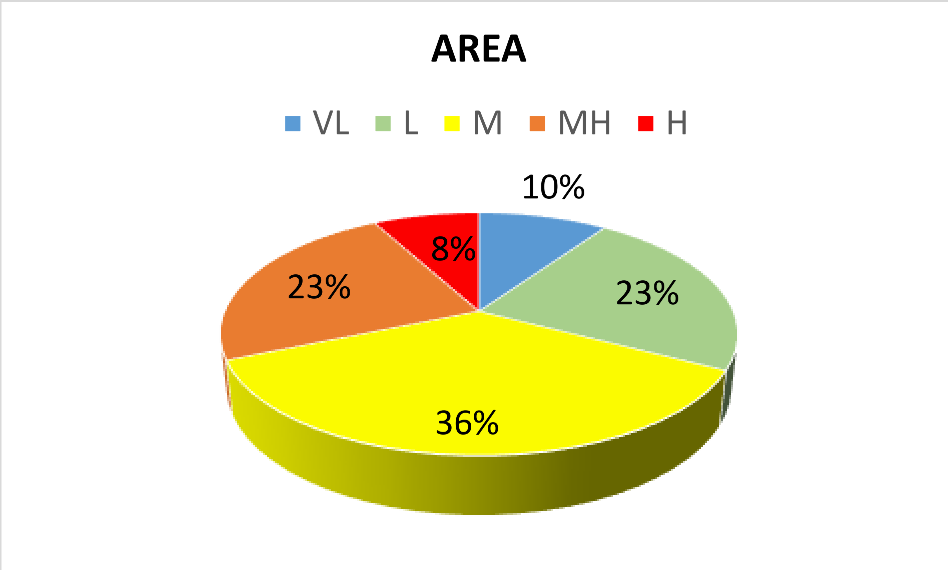

Fig. 12(b): Pie chart showing area coverage of each of the BT classes

4.2. Groundwater vulnerability map

Appropriate groundwater vulnerability classification is necessary for long-term development. Since groundwater is an endangered resource, a number of cultural and environmental factors have been causing its quality to decline. In terms of geographic planning and safety, groundwater vulnerability monitoring is essential. Consequently, the study region's groundwater vulnerability sites have been determined using the findings from the study.

To develop the groundwater vulnerability (GWVB) model for the research area, five distinct conceptually evaluated maps of bedrock topography, hydraulic conductivity, aquifer depth, drainage density, and slope were combined using ArcGIS 10.7 software. The groundwater vulnerability assessment obtained for the IDOCRIW-MAUT model in the researched area was classed as very low (3%), low (26%), medium (33%), medium-high (25%), and high (13%), representing area extents of 59 km², 485 km², 485 km², 464 km², and 251 km², respectively. (**Fig. 13a**). The groundwater vulnerability indicator evaluations map shows that high indexing values, which account for 13% of the study, are located predominantly in the western sections of the studied area, even though isolated areas can be found in the eastern parts. The groundwater vulnerability rating has low-value patches across the research area, including the east, central, north-central, northeastern, and southeastern regions. The northeastern, southern, and central portions of the research area have high groundwater vulnerability index values. In the studied area, the AHP model's classification of groundwater vulnerability was categorized as very low (12%), low (22%), medium (29%), medium-high (27%), and high (10%) (**Fig. 13b**). The groundwater vulnerability indicator evaluation map demonstrates that high indexing values, which account for 10% of the study, are concentrated in the northeast and northwest regions of the study area. In general, the research region has a medium-high to high level of groundwater vulnerability, with the IDOCRIW-MAUT model at 38% and the AHP model at 37% (**Table 11**). The combination of IDOCRIW-MAUT (objective-based) and AHP (subjective-based) provides a diverse set of context-related factors, resulting in multifaceted yet highly accurate techniques for predicting groundwater vulnerability zones in the study area.

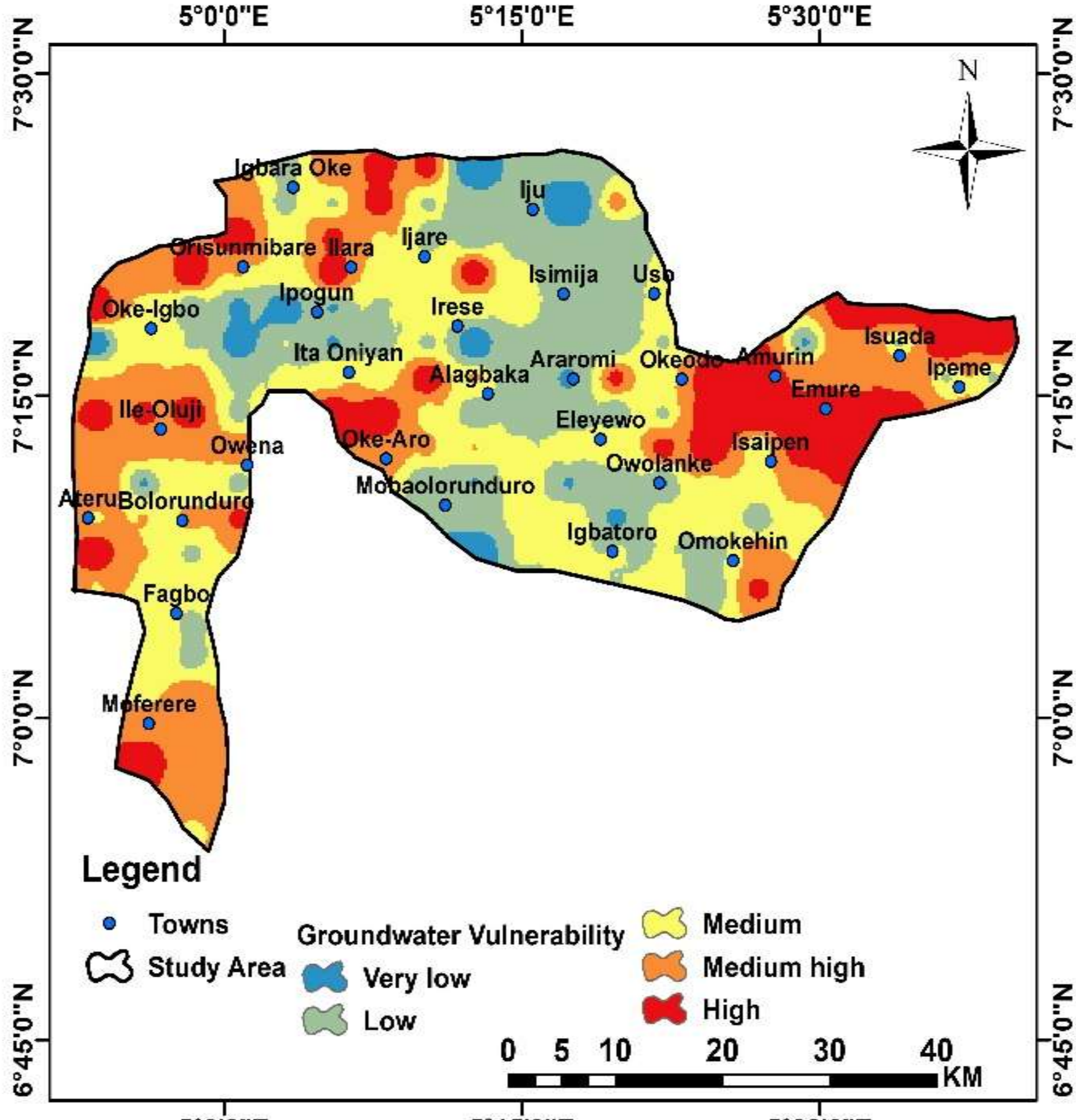

Fig. 13a. IDOCRIW-MAUT groundwater vulnerability model of the study area

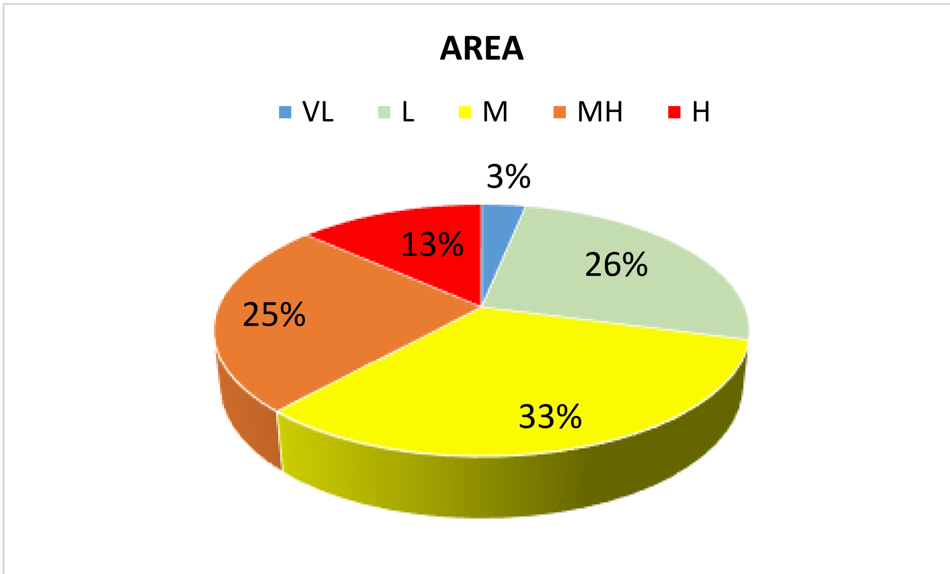

Fig. 12(b): Pie chart showing area coverage of each of the vulnerability classes based on IDOCRIW-MAUT model

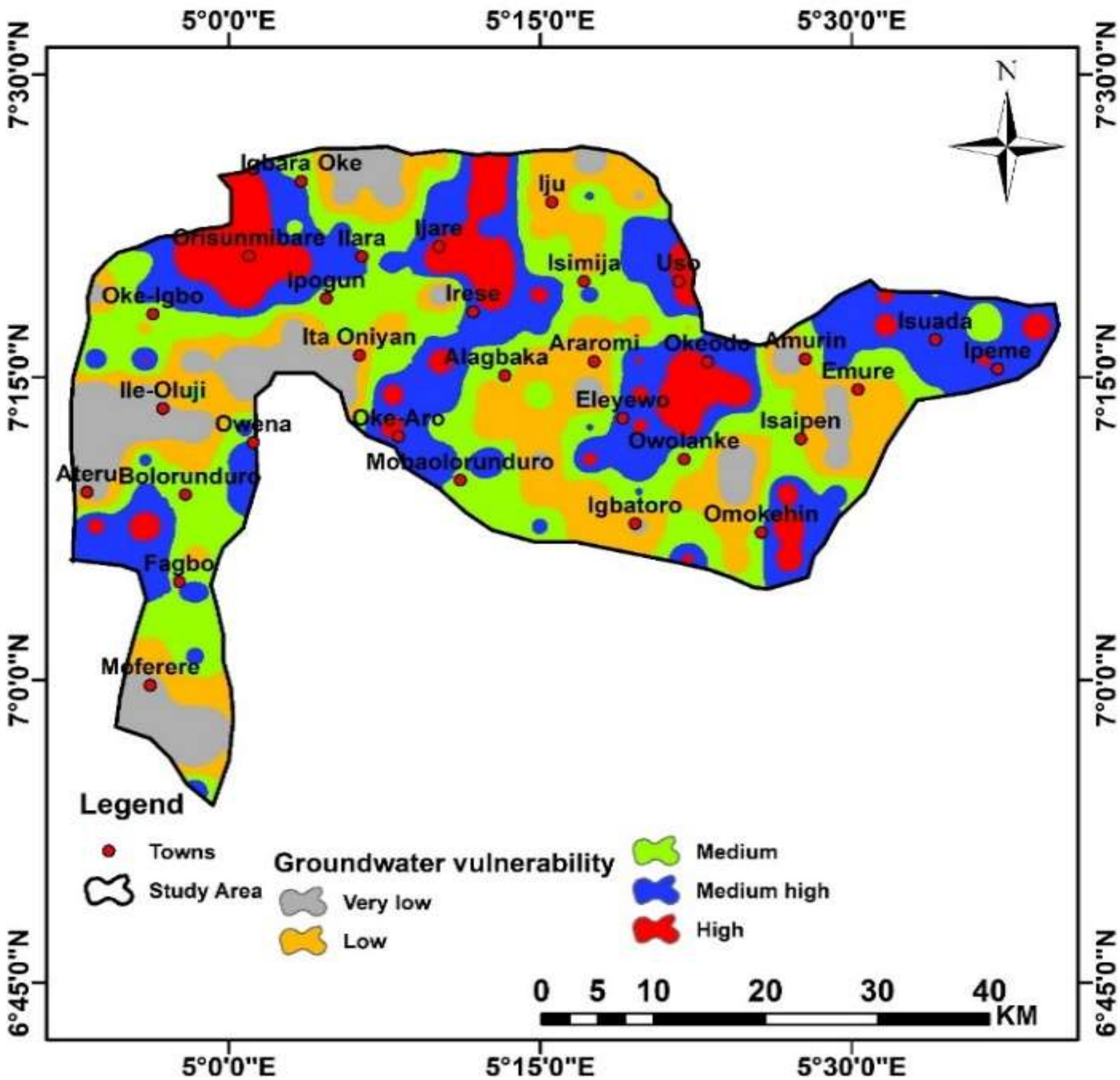

Fig. 13b. AHP groundwater vulnerability model of the study area

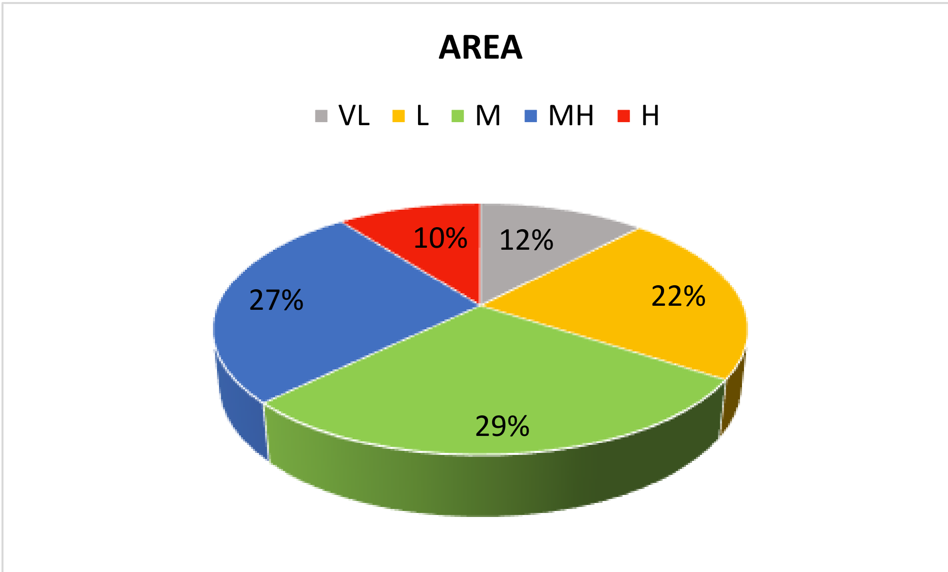

Fig. 12(b): Pie chart showing area coverage of each of the vulnerability classes based on AHP model

Table 11. Result of area classes of groundwater vulnerability based on the IDOCRIW-MAUT and AHP models

Groundwater Vulnerability Classes	Percentage Coverage		Approximate Area Extent	
	IDOCRIW-MAUT	AHP	IDOCRIW-MAUT	AHP
Very low (VL)	3%	12%	59 km^2	224 km^2
Low (L)	26%	22%	485 km^2	411 km^2
Medium (M)	33%	29%	608 km^2	541 km^2
Medium High (MH)	25%	27%	464 km^2	504 km^2
High (H)	13%	10%	251 km^2	187 km^2

4.3. Results validation

4.3.1. Sensitivity analysis outcomes

In the approach, the HC weight is adjusted from 25% to 50% in 5% increments, and the associated criterion weights are then determined in six scenarios (Scenarios 1–6) (**Table 12**). The IDOCRIW-MAUT vulnerability indices for each scenario (**Table S3**) were produced and were then employed in creating a heat map (**Fig. 14**). The heat map was developed by examining the variability of the data in each scenario at the fishnet sites. The data exhibits reduced variations at the majority of the locations, confirming the model's robustness even after adjusting the most critical weight to generate six different scenarios.

Table 12. Criteria weight scenarios upon varying HC weight from 25% to 50% at a step of 5%

Factors	Scenario 1	Scenario 2	Scenario 3	Scenario 0	Scenario 4	Scenario 5	Scenario 6
	HC at 25%	HC at 30%	HC at 35%	Original Value	HC at 40%	HC at 45%	HC at 50%
SL	0.45101	0.42094	0.39087	**0.36525**	0.36081	0.33074	0.30067
DD	0.14068	0.13130	0.12192	**0.11393**	0.11254	0.10317	0.09379
HC	**0.25000**	**0.30000**	**0.35000**	**0.39261**	**0.40000**	**0.45000**	**0.50000**
AD	0.11027	0.10292	0.09557	**0.08930**	0.08821	0.08086	0.07351
BT	0.04804	0.04484	0.04164	**0.03891**	0.03843	0.03523	0.03203

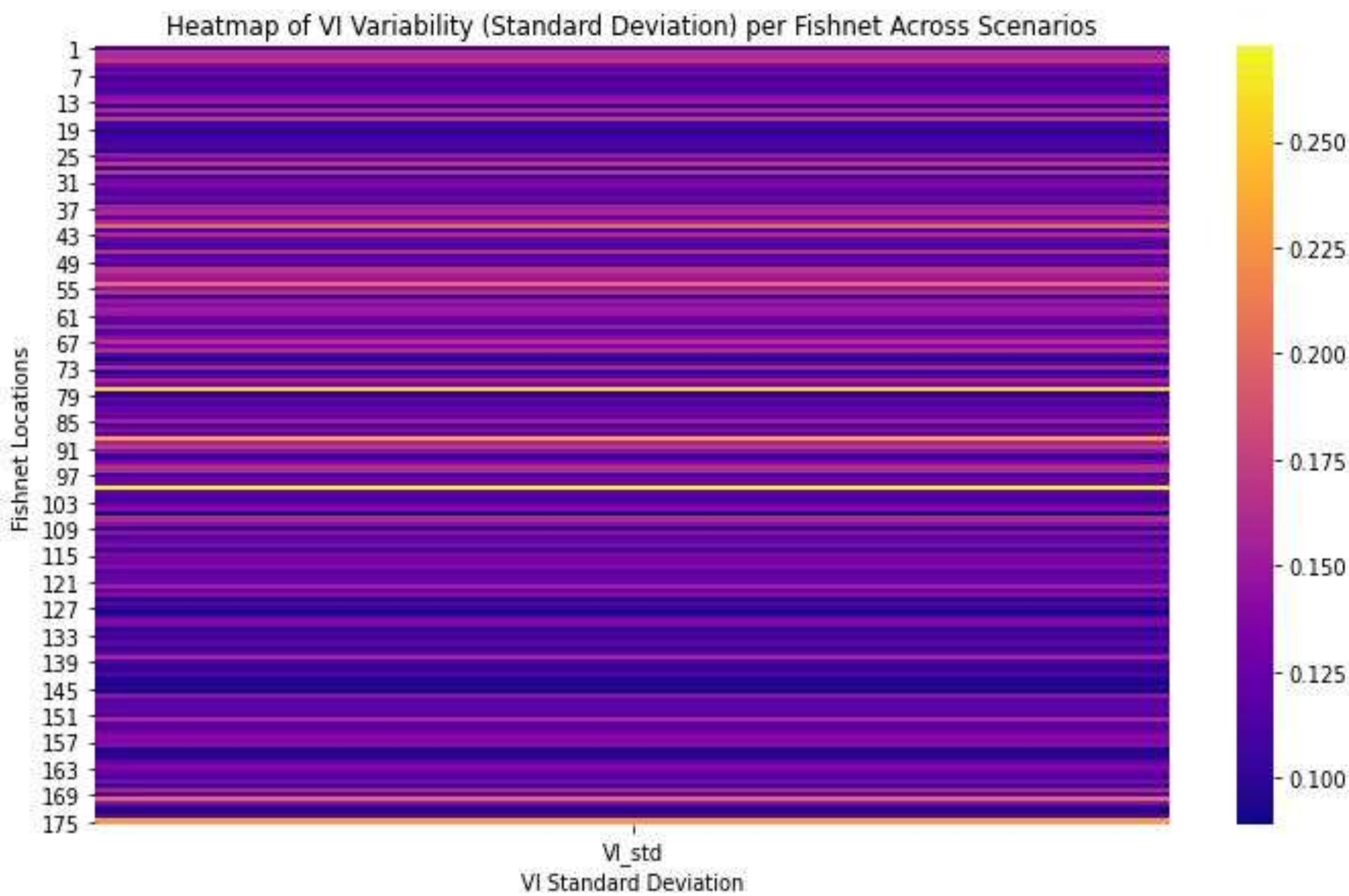

Fig. 14. Heat map of vulnerability indices in the sensitivity analysis of IDOCRIW weight generated

4.3.2. Correlation with LC data

In the context of a study by Oladapo and Akintorinwa (2007) and Atenidegbe and Mogaji (2023), the LC of an aquifer served as a measure of its protective capacity in a correlation means for validating the developed GWVB model maps and assessing the accuracy for ecological decisions. For qualitative validation, the longitudinal conductance data used to create the longitudinal map of the study area (**Fig. 16**) were correlated with the IDOCRIW-MAUT-based groundwater vulnerability indices (VI) as well as the AHP-based vulnerability model using an inverse correlation approach. Prior to this correlation, classification indices of the IDOCRIW-MAUT vulnerability model (**Table 13**) as well as that for the AHP vulnerability model (**Table 13**) and that of LC data were first determined leveraging the Jenks Natural approach used to produce their maps within the GIS software. The inverse correlation approach of the IDOCRIW-MAUT model as well as the AHP model with LC data (**Table 13**) was then performed, and this is required as longitudinal conductance evaluates protective capacity, signifying an inverse relationship with groundwater vulnerability (Agbane et al., 2022).

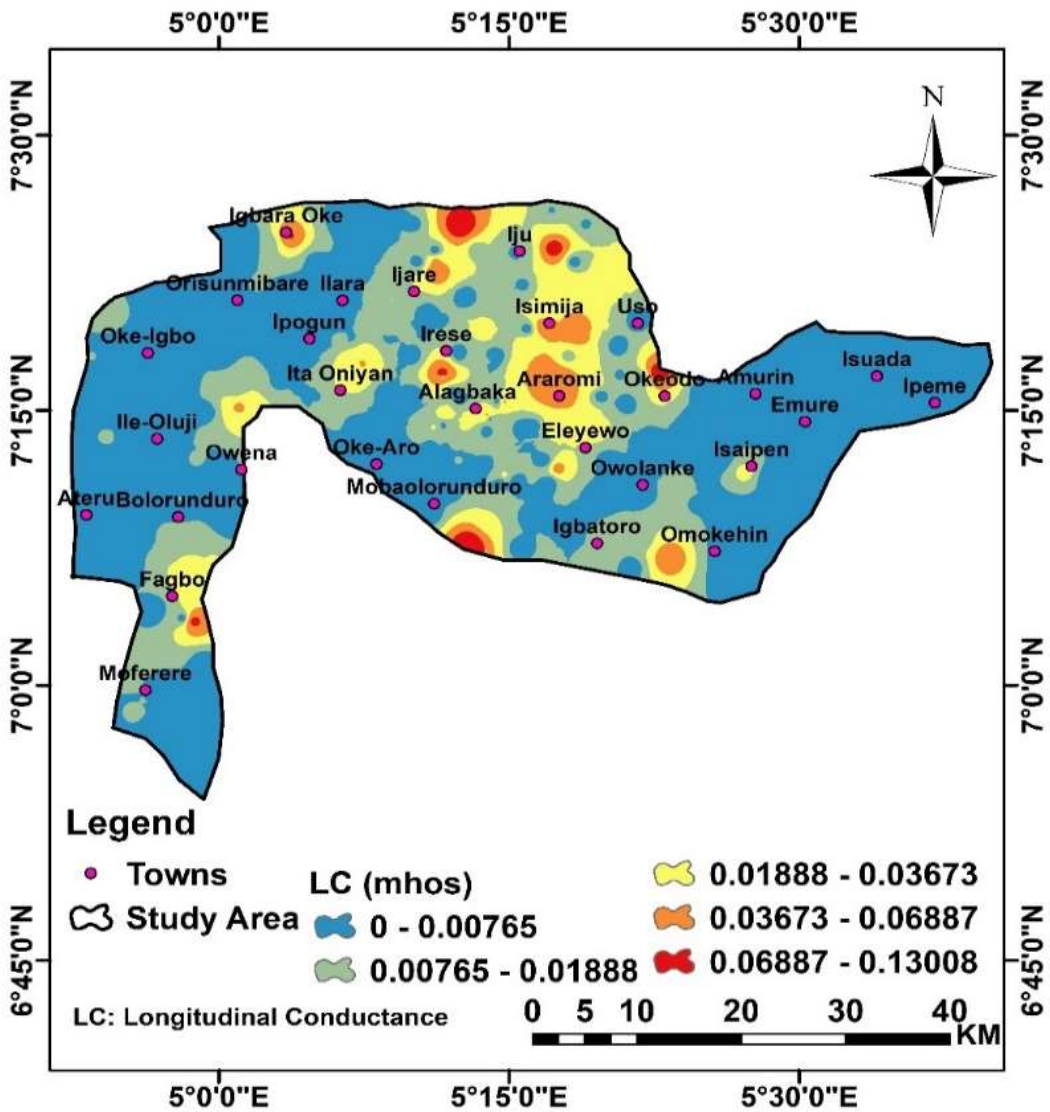

Fig. 16. The vulnerability map showing the indices used for the correlation with LC data

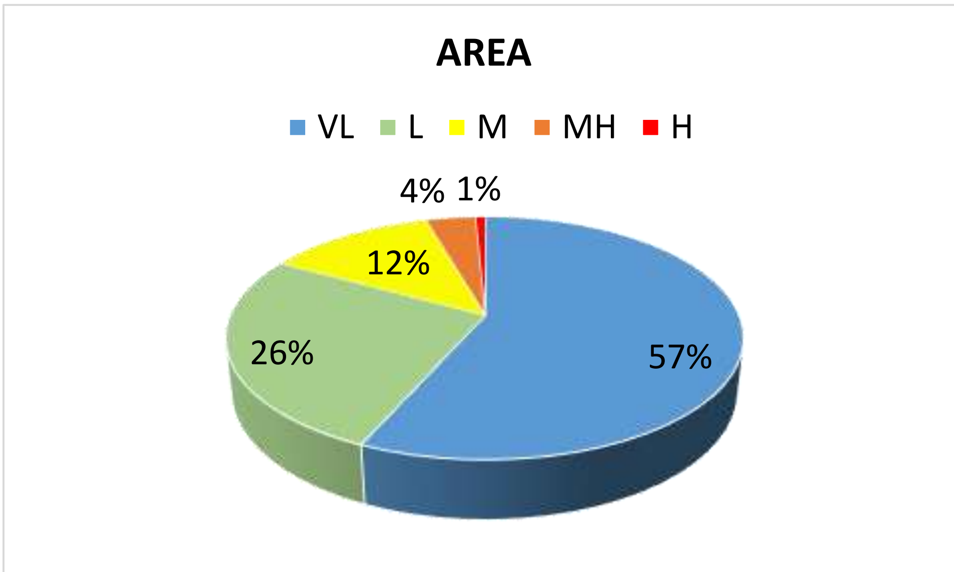

Fig. 16(b): Pie chart showing area coverage of each of the LC classes

Table 13. Classification ranges of LC, IDOCRIW-MAUT GWVBI and AHP-GWVBI

Classification range description	Classification range values		
	LC	**IDOCRIW-MAUT GWVBI**	**AHP-GWVBI**
VL	0.00000 – 0.00765	0.10323 – 0.31116	1.34615 – 2.24778
L	0.00765 – 0.01888	0.31116 – 0.38137	2.24778 – 2.55148
M	0.01888 – 0.03673	0.38137 – 0.43808	2.55148 – 2.79824
MH	0.03673 – 0.06887	0.43808 – 0.52970	2.79824 – 3.06399
H	0.06887 – 0.13008	0.52970 – 0.79184	3.06399 – 3.76631

The following is a study of the quantitative correlation used to calculate the viability rate of the models:

*The correlation result for IDOCRIW-MAUT (**Table S4**) is thus:*

Number of correlated fishnet points = 150

Number of observed fishnet points = 175

Accuracy = 150/175 * 100% = 86%

*Also, leveraging the analysis result presented in **Table S5**, the accuracy of the AHP model is thus:*

Number of correlated fishnet points = 99

Number of observed fishnet points = 175

Accuracy = 99/175 * 100% = 57%

Conclusion

Groundwater susceptibility and threat evaluation are critical for efficient governance of groundwater and safety. The present work assessed groundwater vulnerability in a complex geologic context using the object-oriented multi-criteria decision methods (MCDM) for geophysical and remote sensing data. The object-based MCDM method was applied to 175 equally distributed vantage points across conceptual layers of the study region, addressing groundwater vulnerability influencing parameters. These layers were established geographically, leveraging GIS for processing surface and subsurface data. Python's processing prowess was utilized to lower the cost of generating the conceptual algorithm employed in this research. The IDOCRIW-MAUT index algorithm was used to create the groundwater vulnerability map for the framework. The model predicted areas of extremely low, low, medium, medium-high, and high vulnerabilities within the research area - with the IDOCRIW-MAUT model predicting a 38% medium-high to high level of groundwater vulnerability. Validating the model map with sensitivity analysis and longitudinal conductance of the research area gives greater assurance in the prediction vulnerability model map. The results reveal a better degree of dependability in the established IDOCRIW-MAUT vulnerability index predictive map, validating the efficacy of the proposed model. This study contributes to the advancement of GWVB mapping approaches, providing an improved, dependable, and unbiased procedure for environmental evaluation and conservation initiatives. With increasing human activity and climate unpredictability, this technique has been utilized to offer details about healthy groundwater advancement in relation to land utilization modification and contamination on a regional basis. Notwithstanding its numerous advantages, groundwater vulnerability modelling still faces limitations such as limited data availability, complexities of models, and intrinsic ambiguities. These restrictions can impede the creation of reliable models, especially in areas with insufficient monitoring infrastructure. Overcoming these shortcomings will increase model dependability and advance the processes for making decisions. As increasing populations and climatic changes drive up the need for the availability of groundwater, models must adapt to better describe the intricacies of groundwater vulnerability networks and their associations with surface water bodies and habitats. The created groundwater vulnerability projection maps can be utilized as a reference for groundwater resource managers and prospective regulators in the research area, as well as in other places exhibiting comparable geological conditions that are experiencing polluted groundwater or problems with contaminants.

Appendix

A: Python codes for the computation of IDOCRIW – MAUT model

<u>A1: Entropy weight for GWVBMFs</u>

```python
# import the necessary libraries
import pandas as pd
import numpy as np
# define functions for the calculation process of entropy weights
def normalize_matrix(df):  # normalized data function
    # calculate normalized value of decision matrix
    col_sum = df.sum(axis=0)
    normalized_df = df / col_sum
    return normalized_df
def calculate_entropy(normalized_df):  # entropy calculation function
    # calculate entropy from normalized decision matrix
    log_df = np.log(normalized_df + 1e-12)  # Avoid log(0) by adding a very small value
    entropy_matrix = normalized_df.mul(log_df)
    rows, cols = normalized_df.shape
    k = 1 / np.log(rows)
    entropy = -k * entropy_matrix.sum(axis=0)
    return entropy
def calculate_divergence(entropy):   # divergence function
    # Calculate the degree of divergence (1 - entropy)
    divergence_degree = 1 - entropy
    return divergence_degree
def calculate_weights(divergence):  # entropy weights function
    # Calculate the weights by normalizing the divergence values
    weights = divergence / np.sum(divergence)
    return weights
def entropy_weight(data):     # utilizing the functions
    # read the file as a dataframe by defining a variable data
    df = pd.read_csv(data)
    # call the functions
    normalized_df = normalize_matrix(df)
     # print the normalized decision matrix
    print(normalized_df)
    ## continue with calling the remaining functions
    entropy = calculate_entropy(normalized_df)
    divergence = calculate_divergence(entropy)
    weights = calculate_weights(divergence)
    # Combine the results into a DataFrame
    results_df = pd.DataFrame({
        'Entropy': entropy,
        'Degree of divergence': divergence,
        'Weights': weights
    })

    return results_df
data = 'Entropy_data_gvcf.csv'
results_df = entropy_weight(data)
# print the results
print("Entropy, Degree of Divergence, and Weights for each criterion:")
print(results_df)
```

A2: CILOS weight process to generate weight system matrix for GWVBMFs

```
# import the necessary libraries
import pandas as pd
import numpy as np

# Read the CSV file as a DataFrame
df = pd.read_csv('Cilos_data_gvcf.csv')

# Normalize the decision matrix
normalized_matrix = df / df.sum()

# Convert multiple minimized criteria into maximized ones
# use (minimum_value / value) formula
minimized_columns = ['SL', 'DD', 'AD', 'BT']

for minimized_column in minimized_columns:
    normalized_matrix[minimized_columns] =
normalized_matrix[minimized_columns].min() /
normalized_matrix[minimized_columns]

# Find the largest value in each column and its corresponding row
largest_values = normalized_matrix.max()
row_indices = normalized_matrix.idxmax()

# Create the square matrix A by selecting the rows where the largest values
were found
matrix_A = normalized_matrix.loc[row_indices].values

# Create the relative criterion loss matrix (P)
P = np.zeros(matrix_A.shape)  # Initialize P with zeros

for i in range(matrix_A.shape[0]):
    for j in range(matrix_A.shape[1]):
        if i != j:  # Ensure the diagonal remains zero
            P[i, j] = (largest_values[j] - matrix_A[i, j]) /
largest_values[j]

# Form the weight system matrix (F)
F = np.copy(P)  # Start with F being the same as P
for j in range(P.shape[1]):
    F[j, j] = -np.sum(P[:, j])  # Set the diagonal elements


# Output the results
print("Normalized Decision Matrix:")
print(normalized_matrix)

print("\nLargest values in each column:")
print(largest_values)

print("\nIndices of rows with largest values:")
print(row_indices)

print("\nSquare Matrix A:")
print(matrix_A)

```

```python
print("\nRelative Criterion Loss Matrix (P):")
print(P)

print("\nWeight System Matrix (F):")
print(F)
```

A3: CILOS weight process to solve the weight system matrix and generate the CILOS weights for GWVBMFs

```python
# import necessary libraries
import numpy as np
from scipy.linalg import lstsq

# Matrix F (weight system matrix)
F = np.array([[-2.51724138, 0.64285714, 0.33520337, 0.80236486, 0],
              [0.93103448, -2.71428571, 0.9898317, 0.82094595, 0.52107963],
              [0.86206897, 0.73809524, -2.28786816, 0.75675676, 0.25607852],
              [0.72413793, 0.6904719, 0.62762973, -3.18243243, 0.20231988],
              [0, 0.64285714, 0.33520337, 0.80236486, -0.97947803]])

# Vector B
B = np.array([[0.00037],
              [0],
              [0],
              [0],
              [0]])

# Solve the system of equations F * q = B using least squares
q_vector, residuals, rank, s = lstsq(F, B)

# Calculate weights F
diagonal_abs_values = np.abs(np.diag(F))
weights = 1 / (diagonal_abs_values + 1e-10)  # Add small epsilon to avoid division by zero

# Normalize weights to sum to 1
normalized_weights = weights / np.sum(weights)

# Output the results
print("Unnormalized Solution Vector q (CILOS Weights):")
print(q_vector)

print("\nAbsolute Values of Diagonal Elements in F:")
print(diagonal_abs_values)

print("\nWeights based on Inverse of Diagonal Values:")
print(weights)

print("\nNormalized CILOS Weights:")
print(normalized_weights)
```

A4: IDOCRIW weight for GWVBMFs

```python
# import the necessary library
import pandas as pd
```

```python

# Read the CSV file containing entropy and CILOS weights
weights_df = pd.read_csv('IDOCRIW_data_gvcf.csv')

# Calculate the product of Entropy Weights and CILOS Weights
weights_df['Product'] = weights_df['Entropy_Weights'] *
weights_df['CILOS_Weights']

# Calculate the sum of the products
sum_product = weights_df['Product'].sum()

# Calculate the IDOCRIW Weights
weights_df['IDOCRIW_Weights'] = weights_df['Product'] / sum_product

# Output the resulting IDOCRIW Weights
print("IDOCRIW Weights:")
print(weights_df[['Entropy_Weights', 'CILOS_Weights', 'IDOCRIW_Weights']])

```

<u>A5: IDOCRIW-MAUT algorithm process to generate vulnerability indices</u>

```python
# import the necessary libraries
import numpy as np
import pandas as pd

# Read decision matrix as CSV file
df = pd.read_csv('MAUT_data_gvcf.csv')  # Replace with your actual CSV file
path

# Ensure the data is numeric, coercing non-numeric values to NaN
df = df.apply(pd.to_numeric, errors='coerce')

# Fill NaN values with zeros
df.fillna(0, inplace=True)

# Define maximizing and minimizing criteria columns
maximizing_criteria = ['HC']  # List of column names for maximizing criteria
minimizing_criteria = ['SL','DD','AD','BT']  # List of column names for
minimizing criteria

# Normalize maximizing criteria using (value - min_value) / (max_value -
min_value)
min_values_max_crit = df[maximizing_criteria].min()
max_values_max_crit = df[maximizing_criteria].max()

df[maximizing_criteria] = (df[maximizing_criteria] - min_values_max_crit) /
(max_values_max_crit - min_values_max_crit)

# Normalize minimizing criteria using 1 + (min_value - value) / (max_value -
min_value)
min_values_min_crit = df[minimizing_criteria].min()
max_values_min_crit = df[minimizing_criteria].max()

df[minimizing_criteria] = 1 + ((min_values_min_crit -
df[minimizing_criteria]) / (max_values_min_crit - min_values_min_crit))

# Save the normalized decision matrix to a new CSV file
```

```python
df.to_csv('normalized_maut_matrix.csv', index=False)

# Calculate Marginal Utility
# Read the normalized decision matrix from the CSV file
normalized_df = pd.read_csv('normalized_maut_matrix.csv')

# Define function to calculate marginal utility
def marginal_utility(value):
    return (np.exp(value**2) - 1) / 1.71

# Apply the marginal utility function to each element in the normalized
decision matrix
marginal_utility_matrix = normalized_df.applymap(lambda x:
marginal_utility(x))

# Save the marginal utility matrix to a new CSV file
marginal_utility_matrix.to_csv('marginal_utility_maut_matrix.csv',
index=False)

# Calculate Total Utility
# Read the marginal utility matrix from the CSV file
df = pd.read_csv('marginal_utility_maut_matrix.csv')

# Define the weights for each criterion using a NumPy array
criteria = ['SL', 'DD', 'HC', 'AD', 'BT']  # List of criteria
weights = np.array([0.365249, 0.113930, 0.392613, 0.089300, 0.038908])  #
Corresponding weights as a NumPy array
# Multiply each normalized criterion value by its corresponding weight
weighted_values = df[criteria].values * weights  # Broadcasting to multiply
weights with marginal utility values
df[criteria] = weighted_values  # Update the dataframe with weighted values
df['Total Utility'] = weighted_values.sum(axis=1)  # Sum across rows for
total utility score

# Save the weighted utility DataFrame to a new CSV file
weighted_utility_df = df[criteria]  # Create a DataFrame with only weighted
utility values
weighted_utility_df.to_csv('weighted_utility_dataframe.csv', index=False)  #
Export weighted utility DataFrame

# Save the final results to a new CSV file
df.to_csv('maut_utility_scores.csv', index=False)

# Print results
print("Normalized Decision Matrix:")
print(df)

print("\nMarginal Utility Matrix:")
print(marginal_utility_matrix)

print("\nWeighted Utility DataFrame:")
print(df[criteria])

print("\nFinal Utility Scores for Each Alternative:")
print(df[['Total Utility']])
```

B: Python codes for the generation of AHP-vulnerability indices

```
# AHP weights for Gvcfs

# import the necessary libraries

import numpy as np
import pandas as pd

# Read the pairwise comparison matrix as a CSV file and convert to numpy
array

pairwise_matrix = pd.read_csv('Consolidated_AHP_Pairwise_Matrix_GVCFs.csv',
index_col=0).values

# Square the Pairwise Comparison Matrix
squared_matrix = np.dot(pairwise_matrix, pairwise_matrix)

# Normalize the Squared Pairwise Comparison Matrix
column_sums = np.sum(squared_matrix, axis=0)  # Column-wise sum
normalized_matrix = squared_matrix / column_sums  # Normalize each column

# Compute Row Sums of the Normalized Matrix
row_sums = np.sum(normalized_matrix, axis=1)

# Calculate Criteria Weights
criteria_weights = row_sums / np.sum(row_sums)

# Consistency Check
# Multiply the original matrix by the weights vector
weighted_sum_vector = np.dot(pairwise_matrix, criteria_weights)

# Compute the consistency vector
consistency_vector = weighted_sum_vector / criteria_weights

# Calculate lambda_max
lambda_max = np.mean(consistency_vector)

# Number of criteria (n) and Random Index (RI) values
n = pairwise_matrix.shape[0]
RI_values = {1: 0, 2: 0, 3: 0.58, 4: 0.9, 5: 1.12, 6: 1.24, 7: 1.32, 8: 1.41,
9: 1.45, 10: 1.49}
RI = RI_values.get(n, 1.49)  # Default to max RI if n > 10

# Consistency Index (CI) and Consistency Ratio (CR)
CI = (lambda_max - n) / (n - 1)
CR = CI / RI if RI != 0 else 0

# Output results
print("Pairwise Comparison Matrix (Original):")
print(pairwise_matrix)
print("\nSquared Pairwise Comparison Matrix:")
print(squared_matrix)
print("\nNormalized Matrix:")
print(normalized_matrix)
print("\nCriteria Weights:")
print(criteria_weights)
```

```
print ("\nlambda_max:")
print(lambda_max)
print("\nConsistency Index:")
print(CI)
print(f"\nConsistency Ratio (CR): {CR:.4f}")
```

Acknowledgments

The authors would like to express gratitude to all the experts whose insights have been instrumental to the development of this work. We would also like to thank the anonymous reviewers for their words of expertise that helped refined this work to taste.

References

Abu-Bakr, H.A.E.A., 2020. Groundwater vulnerability assessment in different types of aquifers. Agricultural Water Management, 240, 106275.

Adalı, E.A., Işık, A.T., 2017. CRITIC and MAUT methods for the contract manufacturer selection problem. European Journal of Multidisciplinary Studies 2(5), 88-96.

Adu, J.T., Kumarasamy, M.V., 2018. Assessing non-point source pollution models: a review. Polish Journal of Environmental Studies 27(5).

Agbane, I.O., Agbali, E., Medayese, I.I., Jimoh, J.B., Attah, P.E., Joseph, G.E., Raimi, N., Jolly, P.N., 2022. Aquifer vulnerability and protective capacity test of Lokoja, Kogi state, North-Central Nigeria. International Journal of Applied Chemical and Biological Sciences 3(4).

Akintorinwa, O.J., Atitebi, M.O., Akinlalu, A.A., 2020. Hydrogeophysical and aquifer vulnerability zonation of a typical basement complex terrain: A case study of Odode Idanre southwestern Nigeria. Heliyon 6(8).

Akinwumiju, A.S., Olorunfemi, M.O., 2018. A GIS-based aquifer vulnerability assessment in the basement complex terrain of southwestern Nigeria. Sustainable Water Resources Management 4(4), 715-734.

Alao, M.A., Popoola, O.M., Ayodele, T.R. 2021. Selection of waste-to-energy technology for distributed generation using IDOCRIW-Weighted TOPSIS method: A case study of the City of Johannesburg, South Africa. Renewable Energy 178, 162-183.

Alao, J.O., Ahmad, M.S., Danjumo, T.T., Ango, A., Jaiyeoba, E., 2022. Assessment of aquifer protective capacity, against the surface contamination. A case study of kaduna industrial village, Nigeria. Physical Science International Journal 43-51.

Ali, T., Chiu, Y.R., Aghaloo, K., Nahian, A.J., Ma, H., 2020. Prioritizing the existing power generation technologies in Bangladesh's clean energy scheme using a hybrid multi-criteria decision-making model. Journal of Cleaner Production 267, 121901.

Alinezhad, A., Khalili, J., 2019. New Methods and Applications in Multiple Attribute Decision Making (MADM), International Series in Operations Research & Management Science 277, https://doi.org/10.1007/978-3-030-15009-9_19 133 19.2

Allouche, N., Maanan, M., Gontara, M., Rollo, N., Jmal, I., & Bouri, S., 2017. A global risk approach to assessing groundwater vulnerability. Environmental Modelling & Software 88, 168-182.

Atenidegbe, O.F., Mogaji, K.A., 2023. Modeling assessment of groundwater vulnerability to contamination risk in a typical basement terrain using TOPSIS-entropy developed vulnerability data mining technique. Heliyon 9(7).

Ayan, B., Abacıoğlu, S., Basilio, M.P., 2023. A comprehensive review of the novel weighting methods for multi-criteria decision-making. Information 14(5), 285.

Aziz, Z.A., Abdulqader, D.N., Sallow, A.B., Omer, H.K., 2021. Python parallel processing and multiprocessing: A review. Academic Journal of Nawroz University 10(3), 345-354.

Baki, A.M., Ghavami, S.M., Qureshi, S.A.M., Ghaffari, O., 2024. A three-step modification of the DRASTIC model using spatial multi criteria decision making methods to assess groundwater vulnerability. Groundwater for Sustainable Development 26, 101277.

Bayewu, O.O., Oloruntola, M.O., Mosuro, G.O., Laniyan, T.A., Ariyo, S.O., Fatoba, J.O., 2018. Assessment of groundwater prospect and aquifer protective capacity using resistivity method in Olabisi Onabanjo University campus, Ago-Iwoye, Southwestern Nigeria. NRIAG Journal of Astronomy and Geophysics 7(2), 347-360.

Çetinkaya, C., Erbaş, M., Kabak, M., Özceylan, E., 2023. A mass vaccination site selection problem: An application of GIS and entropy-based MAUT approach. Socio-Economic Planning Sciences 85, 101376.

Chatterjee, S., Lim, S., 2022. A TOPSIS-Inspired Ranking Method Using Constrained Crowd Opinions for Urban Planning. Entropy 24(3), 371. https://doi.org/10.3390/e24030371.

Dangar, S., Asoka, A., Mishra, V., 2021. Causes and implications of groundwater depletion in India: A review. Journal of Hydrology 596, 126103.

Demir, G., Chatterjee, P., Pamucar, D., 2024. Sensitivity analysis in multi-criteria decision making: A state-of-the-art research perspective using bibliometric analysis. Expert Systems with Applications 237, 121660.

Emovon, I., Norman, R. A., Murphy, A.J., 2016. Methodology of using an integrated averaging technique and MAUT method for failure mode and effects analysis. Journal of Engineering and Technology (JET) 7(1), 140–155.

Fannakh, A., Farsang, A., 2022. DRASTIC, GOD, and SI approaches for assessing groundwater vulnerability to pollution: a review. Environ. Sci. Eur. 34, 77. https://doi.org/10.1186/s12302-022-00646-8.

Erostate, M., Huneau, F., Garel, E., Ghiotti, S., Vystavna, Y., Garrido, M., Pasqualini, V., 2020. Groundwater dependent ecosystems in coastal Mediterranean regions: Characterization, challenges and management for their protection. Water research 172, 115461.

Frye, C., Wright, D. J., Nordstrand, E., Terborgh, C., Foust, J., 2018. Using classified and unclassified land cover data to estimate the footprint of human settlement. Data Science Journal 17, 20-20.

Gernez, S., Bouchedda, A., Gloaguen, E., Paradis, D., 2019. Comparison between hydraulic conductivity anisotropy and electrical resistivity anisotropy from tomography inverse modeling. Frontiers in Environmental Science 7, 67.

Gorelick, S.M., Zheng, C., 2015. Global change and the groundwater management challenge. Water Resources Research 51(5), 3031-3051.

Ilugbo, S.O., Aigbedion, I., Ozegin, K.O., Bawallah, M.A., 2023. Assessment of groundwater occurrence in a typical schist belt region in Osun state, southwestern Nigeria using VES, aeromagnetic dataset, remotely sensed data and MCDA approaches. Sustain. Water Resourc. Manag. 9, 29. https://doi.org/10.1007/s40899-022-00810-1.

Isah, A., Bassey, E.N., Akinbiyi, O.A., Azeez, R.A., Oji, A.S., El-Badawy, T., 2025. Characterizing groundwater contamination flow-paths and heavy metal mobilization near a waste site in Southwestern Nigeria. Journal of African Earth Sciences, 221, 105460.

Işik, Ö, Koşaroğlu, Ş.M., 2020. Analysis of the financial performance of Turkish listed oil companies through the application of SD and MAUT methods. Third Sector Social Economic Review 55(3), 1395-1411. https://doi.org/10.15659/3.sektor-sosyal-ekonomi.20.06.1378.

Jia, Y., Xi, B., Jiang, Y., Guo, H., Yang, Y., Lian, X., Han, S., 2018. Distribution, formation and human-induced evolution of geogenic contaminated groundwater in China: A review. Science of the total environment 643, 967-993.

Kayode, M.O., Adiat, K.A.N., Tomori, W.B., Okoronkwo, E.A., Afolabi, D.O., 2024. Aquifer Vulnerability Assessment of Groundwater in a Basement Complex Geology Using Fuzzy Analytical Hierarchy Process. Asian Journal of Geological Research. 7(3), 331-50. https://journalajoger.com/index.php/AJOGER/article/view/175.

Keeney, R. L., Raiffa, H., 1993. Decisions with multiple objectives: preferences and value trade-offs. Cambridge university press.

Kellogg, K.S., Shroba, R.R., Ruleman, C.A., Bohannon, R.G., McIntosh, W.C., Premo, W.R., Brandt, T.R., 2017. Geologic map of the upper Arkansas River valley region, north-central Colorado (No. 3382). US Geological Survey.

Köpp, C., von Mettenheim, H.J., Breitner, M.H., 2014. Decision Analytics with Heatmap Visualization for Multi-step Ensemble Data: An Application of Uncertainty Modeling to Historical Consistent Neural Network and Other Forecasts. Business & Information Systems Engineering 6, 131-140.

Kumar, P., Sharma, R., Bhaumik, S., 2022., MCDA techniques used in optimization of weights and ratings of DRASTIC model for groundwater vulnerability assessment. Data Science and Management 5(1), 28-41.

Kumar, P., Sharma, R., Bhaumik, S., 2022. MCDA techniques used in optimization of weights and ratings of DRASTIC model for groundwater vulnerability assessment. Data Science and Management 5(1), 28-41.

Li, P., Karunanidhi, D., Subramani, T., Srinivasamoorthy, K., 2021. Sources and consequences of groundwater contamination. Archives of environmental contamination and toxicology 80, 1-10.

Margat J., van der Gun J., 2013 Groundwater around the world: a geographic synopsis. Taylor & Francis Group, London

Mogaji, K.A., Atenidegbe, O.F., 2023. Development of PROMETHEE-Entropy data mining model for groundwater potentiality modeling: a case study of multifaceted geologic settings in south-western Nigeria. Acta Geophysical 1-28.

Mogaji, K.A., Lim, H.S., 2017. Groundwater potentiality mapping using geoelectrical-based aquifer hydraulic parameters: A GIS-based multi-criteria decision analysis modeling approach. Terr. Atmos. Ocean. Sci, 28, 479-500.

Mokarram, M., Mokarram, M.J., Gitizadeh, M., Niknam, T., Aghaei, J., 2020. A novel optimal placing of solar farms utilizing multi-criteria decision-making (MCDA) and feature selection. J. Clean. Prod. 261, 121098

Murray, A., 2015. A method for characterizing basement rocks from borehole images. Geological Society, London, Special Publications 421(1), 109-124.

Neshat, A., Abed, M., Ramezani, M., 2024. Assessment of groundwater vulnerability to pollution based on new hybrid approach methods. Water and Irrigation Management 14(2), 291-308.

Oladapo, M.I., Akintorinwa, O.J., 2007. Hydrogeophysical study of ogbese south western Nigeria. Global journal of pure and applied sciences 13(1), 55-61.

Olajide, A., Bayode, S., Fagbemigun, T., Oyebamiji, A., Amosun, J., Owasanoye, A., 2020. Evaluation of aquifer protective capacity and groundwater potential in part of Iju, Akure-North, Ondo State, Nigeria. Journal of the Nigerian society of Physical Sciences 197-204.

Olaseeni, O.G., Oladapo, M.I., Olayanju, G.M., 2021. Vulnerability assessment of an aquifer in the basement complex terrain of Nigeria using 'LAHBUD'model. Modeling Earth Systems and Environment 7, 833-852.

Omonijo, A.G., Matzarakis, A., 2011. Climate and bioclimate analysis of Ondo State, Nigeria. Meteorologische Zeitschrift, 20(5), 531.

Ozegin, K.O., Ilugbo, S.O., Ogunseye, T.T., 2023. Groundwater exploration in a landscape with heterogeneous geology: an application of geospatial and analytical hierarchical process (AHP) techniques in the Edo north region, in Nigeria. Groundwater for Sustainable Development 20, 100871. https://doi.org/10.1016/j.gsd.2022.100871.

Ozegin, K.O., Ilugbo, S.O., Alile, O.M., Iluore, K., 2024a. Integrating in-situ data and spatial decision support systems (SDSS) to identify groundwater potential sites in the Esan plateau, Nigeria. Groundwater for Sustainable Development 26, 101276. https://doi.org/10.1016/j.gsd.2024.101276.

Ozegin, K.O., Ilugbo, S.O., Adebo, B., 2024b. Spatial evaluation of groundwater vulnerability using the DRASTIC-L model with the analytic hierarchy process (AHP) and GIS approaches in Edo State, Nigeria. Phys. Chem. Earth 134, 103562. https://doi.org/10.1016/j.pce.2024.103562.

Ozegin, K.O., Ilugbo, S.O., Akande, O.N., 2024c. Leveraging geospatial technology and AHP for groundwater potential zonation in parts of south and north-Central Nigeria. Sustainable Water Resources Management. 10, 146. https://doi.org/10.1007/s40899-024-01124-0.

Parameshwaran, R., Kumar, S. P., Saravanakumar, K., 2015. An integrated fuzzy MCDM based approach for robot selection considering objective and subjective criteria. Applied Soft Computing 26, 31-41.

Rahaman, M.A., 1988. Review of the Basement Geology of S.W Nigeria. Geology of Nigeria 1, 39-56

Rajput, H., Goyal, R., Brighu, U., 2020. Modification and optimization of DRASTIC model for groundwater vulnerability and contamination risk assessment for Bhiwadi region of Rajasthan, India. Environmental Earth Sciences 79, 1-15.

Saaty, R.W., 1987. The analytic hierarchy process—what it is and how it is used. Mathematical modelling, 9(3-5), 161-176.

Saaty, T.L. 2008. Decision making with the analytic hierarchy process. International journal of services sciences, 1(1), 83-98.

Saaty, T.L., Ozdemir, M.S., 2021. The Encyclicon-Volume 1: A dictionary of decisions with dependence and feedback based on the analytic network process. RWS Publications.

Şahin, M., 2021. Location selection by multi-criteria decision-making methods based on objective and subjective weightings. Knowledge and Information Systems 63(8), 1991-2021. https://doi.org/10.1007/s10115-021-01588-y.

Şahin, M., 2021. Comprehensive analysis of weighting and multicriteria methods in the context of sustainable energy. Int J Environ Sci Technol, 18(6), 1591-1616. https://doi.org/10.1007/s13762-020-02922-7.

Sahoo, S.K., Goswami, S.S., 2023. A comprehensive review of multiple criteria decision-making (MCDM) Methods: advancements, applications, and future directions. Decision Making Advances 1(1), 25-48.

Saqr, A.M., Ibrahim, M.G., Fujii, M., Nasr, M., 2021. Sustainable development goals (SDGs) associated with groundwater over-exploitation vulnerability: geographic information system-based multi-criteria decision analysis. Natural Resources Research 30, 4255-4276.

Şener, E, Şener, Ş., Davraz, A., 2018. Groundwater potential mapping by combining fuzzy-analytic hierarchy process and GIS in Beyşehir Lake Basin, Turkey. Arabian Journal of Geosciences, 11(8), 187. https://doi.org/10.1007/s12517-018-3510-x.

Tavakoli, M., Motlagh, Z. K., Sayadi, M. H., Ibraheem, I. M., Youssef, Y.M., 2024. Sustainable Groundwater management using machine learning-based DRASTIC model in Rurbanizing riverine region: A case study of Kerman Province, Iran. Water 16(19), 2748. https://doi.org/10.3390/w16192748.

Tijani, M.N., Obini, N., Inim, I.J., 2021. Estimation of aquifer hydraulic parameters and protective capacity in basement aquifer of south-western Nigeria using geophysical techniques. *Environmental Earth Sciences*, *80*, 1-19.

Tolche, A.D., 2021. Groundwater potential mapping using geospatial techniques: a case study of Dhungeta-Ramis sub-basin, Ethiopia. Geology, Ecology, and Landscapes 5(1), 65-80.

Trinkuniene, E., Podvezko, V., Zavadskas, E. K., Joksiene, I., Vinogradova, I., Trinkunas, V., 2017. Evaluation of quality assurance in contractor contracts by multi-attribute decision-making methods. Economic Research (Ekonomska Istrazivanja) 30(1), 1152–1180.

Velis, M., Conti, K. I., Biermann, F., 2017. Groundwater and human development: synergies and trade-offs within the context of the sustainable development goals. Sustainability science 12, 1007-1017.

Vinogradova, I., Podvezko, V., Zavadskas, E. K., 2018. The recalculation of the weights of criteria in MCDM methods using the bayes approach. Symmetry 10(6), 1–18.

Von Neumann, J., Morgenstern, O., 2007. Theory of games and economic behavior: 60th anniversary commemorative edition. In Theory of games and economic behavior. Princeton university press.

Vouillamoz, J.M., Lawson, F.M.A., Yalo, N., Descloitres, M., 2015. Groundwater in hard rocks of Benin: Regional storage and buffer capacity in the face of change. Journal of Hydrology 520, 379-386.

Wang, S., Wang, Y., Wang, Y., Wang, Z., 2022. Assessment of influencing factors on non-point source pollution critical source areas in an agricultural watershed. Ecological Indicators 141, 109084.

Wang, X. J., Zhang, J. Y., Shahid, S., Guan, E. H., Wu, Y. X., Gao, J., He, R. M., 2016. Adaptation to climate change impacts on water demand. Mitigation and Adaptation Strategies for Global Change, 21, 81-99.

Wells, R., Haugerud, R.A., Niem, A.R., Niem, W.A., Ma, L., Evarts, R.C., Sawlan, M. G., 2020. Geologic map of the greater Portland metropolitan area and surrounding region, Oregon and Washington (No. 3443). US Geological Survey.

Zare, M., Nikoo, M. R., Nematollahi, B., Gandomi, A.H., Farmani, R., 2023. Multi-variable approach to groundwater vulnerability elucidation: A risk-based multi-objective optimization model. Journal of Environmental Management 338, 117842.

Zavadskas, E. K., Podvezko, V., 2016. Integrated determination of objective criteria weights in MCDM. International Journal of Information Technology & Decision Making 15(02), 267-283.

Zavadskas, E. K., Cavallaro, F., Podvezko, V., Ubarte, I., Kaklauskas, A., 2017. MCDM assessment of a healthy and safe built environment according to sustainable development.